Nanoscale

Accepted Manuscript

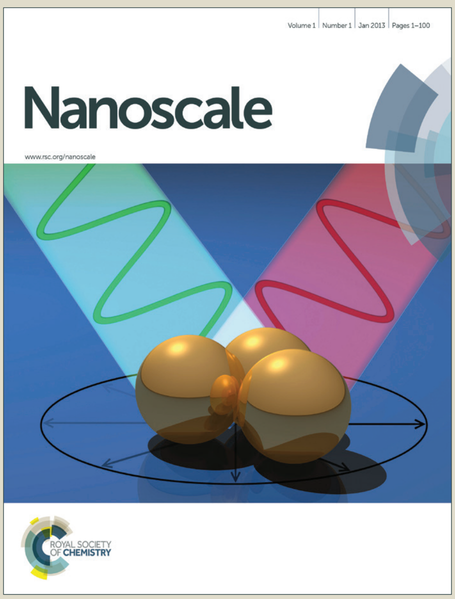

Recent developments and directions in printed nanomaterials†

Hyung Woo Choi,[a], Tianlei Zhou,[a] Madhusudan Singh,[b‡] and Ghassan E. Jabbour[*c,a]

Received Xth XXXXXXXXXX 20XX, Accepted Xth XXXXXXXXX 20XX
First published on the web Xth XXXXXXXXXX 20XX
DOI: 10.1039/b000000x

In this review, we survey several recent developments in printing of nanomaterials for contacts, transistors, sensors of various kinds, light-emitting diodes, solar cells, memory devices, and bone and organ implants. Commonly used nanomaterials are classified according to whether they are conductive, semiconducting/insulating or biological in nature. While many printing processes are covered, special attention is paid to inkjet printing and roll-to-roll printing in light of their complexity and popularity. In conclusion, we present our view of the future development of this field.

1 Introduction

Additive fabrication process offer a thematic contrast to traditional micro-fabrication processes that rely critically on subtractive patterning. While semiconductor growth is intrinsically a bottom-up process where multi-scale additions of material, at atomic, molecular, grain, region and layer, are successively grown, processing of exploitable devices involves several steps: a) formation of device regions composed of uniquely defined materials, b) formation of any contact regions needed to access the device electrically, c) formation of any optical in- or out-coupling regions, d) design of the process steps in a way that avoids compromising any previously defined material regions.

This process has traditionally been carried out in top-down method, with definition of patterns of different material regions at ever shrinking length scales. A complex process employed in micro-fabrication may involve lithography, development, etching, in addition to additive steps such as oxidation, spin-coating (usually of photoresist), and chemical vapour deposition.[1] The benefits of this process, namely, accurate control over device dimensions, scalability to high-volume manufacture, use of a native oxide and other suitable dielectrics and very large scale integration of devices on a single chip, have revolutionized electronics and optoelectronics in recent decades.

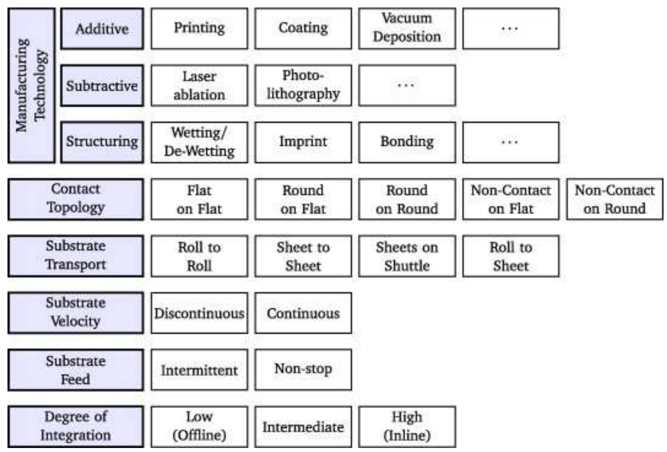

Fig. 1 A classification of various manufacturing processes of potential relevance to device fabrication. Reproduced with permission.[6]

An alternate process, which involves a class of bottom-up methods[2–5] like self-assembly, involves the assembly of complex structures through assembly of atoms/molecules to form predefined shapes at ever-increasing length-scales. While in relative infancy, recent progress has been rapid. A recent work[6] comparing various variants of substrate transport based fabrication processes provides a plausible classification (Fig. (1)) of fabrication processes. Various fabrication methods differ from each other on the basis of the nature of contact topology, abstract notions of substrate handling, substrate motion in relation to the motion on the production like, production scheduling, and the overall degree of integration. Given the scope of this review article, it is instructive to examine different printing processes in a unified manner using this classification.

Nanomaterials are ideal additive building blocks for addi-

† Electronic Supplementary Information (ESI) available: [details of any supplementary information available should be included here]. See DOI: 10.1039/b000000x/

[a] *Department of Chemical and Materials Engineering, University of Nevada, Reno, NV, 89557, United States.*
[b] *Functional Materials and Devices Laboratory, Department of Electrical Engineering, Indian Institute of Technology Delhi, Hauz Khas, New Delhi, India - 110 016*
[c] *Renewable Energy Center, University of Nevada, Reno, NV, 89557, United States. Tel: +1-775-784-1603. Fax: +1-775-327-5059. E-mail: ghassan.jabbour@unr.edu*

tive processes[7,8] as they permit precise control over material properties, high purity through synthesis-dependent methods, selective collapse of dimensional symmetry, confinement of carrier wavefunctions,[9] and resulting change in properties, growth methods attuned to dimensionality of such material systems, control of extent and nature of *interconnection* between nanomaterials[10] that permit different kinds of material aggregation at different length scales, and thus permit expression of different emergent material properties and device performance.[11] The design of material properties possible through intelligent use of synthesis and fabrication methods is not accessible otherwise without radical changes in the fundamental chemistry of constituent substances, something that is not always possible. Thus, while superficially, aggregation of materials at length scales of relevant devices is the first apparent benefit of combining additive processes like printing with nanomaterials, the economies of scale in the process, the development of mesoscale properties and unique device architectures[12] presents an endless variety of choices of device fabrication routes and obviates several processing limitations otherwise inherent in top-down or subtractive manufacturing.[13]

2 Printing methods

While not strictly classifiable as bottom-up fabrication processes, printing processes (with some exceptions) are additive in nature and thus are similar in spirit to these bottom-up processes at larger length scales. Traditional printing in laboratory research involves the ejection of a (usually) liquid ink out of a cartridge in the form of controllable drops, the impact of the drop on the desired substrate, and its subsequent motion under the joint influence of surface tension interaction with the substrate influencing the initial radially outward motion, evaporation of the solvent comprising the ink, time-dependent viscosity of the variable mass ink system and interaction with the ambient in terms of temperature and humidity.[14–16] A slight departure on this process has gained prominence in recent years in the form of three-dimensional printing which involves a layer by layer construction of three-dimensional objects using cross-sections derived from a three-dimensional model of the object, and employing a binder material. It is possible to look at inkjet printing, which is described next, as an exemplar 3D printing process if the ink can be immobilized on the substrate quickly, and added ink preferably deposits new material vertically instead of spreading out horizontally.[17] In this section, we will briefly survey two main printing methods - inkjet/3D printing and roll-to-roll printing and related processes. This choice is based on the relative complexity of these two printing processes. Other printing methods like screen printing,[18] gravure printing / imprinting,[19–21] flexographic printing,[19,22–24] etc. find extensive applications, and are referenced in the remainder of this review as needed. The reader is advised to consult the cited literature on the subject to become familiar with these closely allied processes.

2.1 Inkjet printing

Like laser-based direct write methods, such as femtosecond laser ablation,[25] and laser decal transfer,[26] volatile liquid-based printing methods can employ a variety of materials, depending on the nature of the printing process and what is sought to be printed.[14,27] While either solution- or suspensions-based inks can be printed, these choices correspond to certain unique features, and limitations in actual practice.

Solution-based inks, depending upon the volatility of the solvent used, and the viscosity of the ink, can provide a simpler and more deterministic print recipe design once the rheological properties of the ink are known and the environment suitably controlled. However, the solubility of the materials sought to be deposited is controlled by the nature of the solvent, temperature, humidity and ink pH. This combination of factors can limit overall weight loading and result in various film non-idealities upon drying, such as cracking upon volume contraction, intrinsic stress and in extreme cases, peeling off or delamination. An ideal solution-based ink and its deposition process would contain a sufficient loading of the solute and be dried in a manner that preferentially densifies at the substrate-ink interface, thereby avoiding volumetric cracking. In geometric terms, such a process could be triggered to precipitate the solute through exceeding the solubility limits controllably in a localized region of the ink column above the substrate. A temperature gradient between the cartridge printing the ink and the substrate, for instance, could accomplish this task. On the other hand, use of suspension-based inks, which may involve use of colloidal suspensions, nanoparticles permits the ink designer to exceed solubility limits greatly, thereby increasing weight loading and producing more stable films. However, such suspensions can be unstable and thus have a fixed shelf-life beyond which precipitation and aggregation becomes appreciable. In both cases, the process designer must contend with the tendency of the printed ink to form ring stains, or central spikes due to capillary[28] or Marangoni[29] flows during the drying of the ink drop, to different extents.

A recently demonstrated direct writing technique exploits the capillary effect in conjunction with a rollerball pen.[30,31] In traditional inkjet printing systems based on piezoelectric heads, the feature size that can be printed is closely related to the size of the droplet that can be ejected, and surface treatments of substrates[27,32–34]. Further, the droplet size is also a strong function of the nozzle diameters. The effect of the jet velocity, v, orifice diameter, d, surface tention, σ, and density of the ink, ρ. We can define the Ohnesorge (Oh) number for a print process, as,

$$Oh = \frac{\sqrt{We}}{Re} = \frac{\eta}{\sqrt{\sigma \rho d}} \quad (1)$$

where We, and Re are the Weber and Reynolds numbers for the flow, respectively. It is known that to avoid satellite drop formation and ensure printability, Oh must lie between 0.1 and 1. This dimensionless figure of merit, though used in careful ink design, is in actual practice mirrored by a practical knowledge of ink formulations, and jetting waveform design.

While picoliter level volume control is readily attainable using piezoelectric cartridges in conjunction with inkjet printing, the desire to access ever finer feature sizes has resulted in the development of subfemtoliter inkjet printing systems based on electrohydrodynamic (EHD) jet printing.[35,36] The pulsing frequency[37] is found to exert a strong influence in the formation of ink droplets as exhibited in Fig. (2). The authors[37] found that with increasing frequency, droplets formed reduced in size (and size variability), which would be expected to decrease the size of minimum feature printed. However, this decrease was accompanied by an increase in the impact velocity of the droplet on the substrate, which in turn is expected to degrade the quality of the print. The placement accuracy of the drop is governed by the width of the jet and the resolution provided by the moving stage.[38,39] The diameter of the jet has been found to be proportional to the square root of the nozzle size and inversely proportional to the electric field.[40] Earlier studies have indicated that it is possible to access very fine dot-like features (~ 240 nm) using EHD-based printing methods.[35] There are several reports on line-widths and three dimensional features in the range of 1-20 μm.[40–42] Applications of this increasingly popular process include electrospinning of polymers using a direct writing technique.[43]

Solution-based processes like printing lends themselves naturally to large area deposition of various dissolved species or suspensions. While the performance of solution-deposited devices lags slightly behind devices fabricated using more conventional micro-fabrication methods, the gap in performance has narrowed in recent years.[45] This encouraging improvement in device performance has opened up stronger prospects of industrial adoption of printing processes as preferred low-cost fabrication. As a process based on extensive use of solvents which are volatile, or have to be disposed after use, it is essential that the best practices in inkjet printing be informed by our latest understanding of green chemistry.[46,47] $\pi^* - \beta$, or Kamlet-Taft plots for solvents are used to systematise the search for solvents depending on the application. However, beyond basicity and polarity, other parameters of a solvent, such as boiling point, viscosity, surface tension, solu-

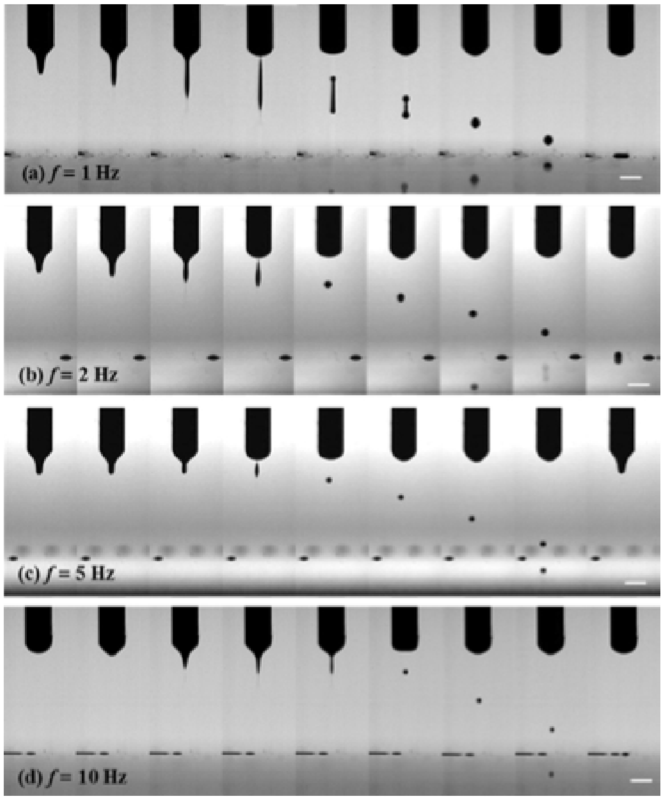

Fig. 2 EHD silver ink droplet ejection as a function of frequency. Time interval=1 ms, scale bar = 1 mm. Reproduced with permission.[44]

bility, density, and specific gravity are also relevant to a print process, as are the mathematical quantities defined in Eq. (1). This shrinks the corresponding *solution* space even further[46], making it a particularly difficult challenge to meet. It is essential to realize that given the sensitivity of printing processes on the choice of the solvent, a resolution of this problem cannot be deferred as an industry-specific problem of little interest to scientists in the lab. In this light, recent work has explored the use of non-halogenated solvents for large area OLED and OSC applications of polymer printing.[48] A new strategy turns the traditional idea of high-boiling point solvents with high solubility on its head by combining a volatile, high solubility solvent with a stable, low solubility solvent.[49] The effect of such a choice on the throughput of device fabrication is as yet unexplored.

If the ink used in an inkjet printing process can be made significantly more viscous or the printed material can otherwise be quickly immobilized on the surface instead of undergoing capillary[28] or Marangoni flow,[29] material growth occurs preferentially in the vertical direction as opposed to formation of relatively thin layers. This regime of printing can technically be referred to as 3D printing. In practical 3D printers, binder elements (as in fused deposition modelling) are added to provide the binding force between the material sought to be printed as well as the higher viscosity needed to suppress lateral expansion of the droplet. Though the process is more than 40 years old[50], significant price drops after 2010 and availability of easy to use software has pushed this technology into teaching, research, and importantly, hobby-craft.[51,52] Unsurprisingly, market trends have followed suit.[53,54] Due to the rapidly expanding range of applications of conventional printing processes[14,55–57], extensions of the achievements with conventional printing processes have begun to be replicated in the third dimension as well.[58] One of the most common applications of 3D printing involve creation of rapid prototypes that can be used for casting or heat pressing.[59] Historically, initial work done by the Evans group on direct inkjet printing has involved printing or ceramic-based[60,61] and wax-based oxide[62] suspensions, and 3D growth of vertical walls.[63]

One of the major disadvantages of 3D printing is the deviation from design lengths due to composition-dependent volumetric changes in the polymer-binder as it dries after the print (*bleeding effect*). When the size of the printed object reduces, there is need for a more intelligent software that can take the drying properties of the ink into account and design around it.[64–67] Contrary to expectations from the historical market response to expiry of patents, such as the fused deposition modeling patent (FDM) which expired in 2009, the more recent expiry of the selective laser sintering patent in January 2014 has not yet led to an exponential growth in open source/hardware solutions corresponding to that technology,[68] thought one may reasonably expect greater growth in the years to come.

2.2 Roll-to-roll printing

Methods of printing corresponding to the graphics arts industry, such as newsprint, banner and textile printing, are expected to maximize the throughput of large-area flexible device fabrication. While alternatives to it exist,[6] a common method used in this context is roll-to-roll (R2R) printing. Such methods are extensively used applications where production of large area devices is prominent. Growing interest in wearable devices, such as sensors[69] integrated into textiles, has further enhanced the potential uses of this process. Applications of roll-to-roll processing include, deposition of electrodes,[70–73], sensors,[74,75], polymer FETs,[76] optical films,[77] and most importantly, large-area solar cells.[19,22,23,78–84] R2R methods can be combined nearly seamlessly with other industrially scaleable processes such as chemical vapour deposition (CVD),[85] sputtering,[86] and address small feature sizes accessible during UV-imprint,[87] and nano-imprint[88] lithography. Conventional application of R2R process has involved single thin film deposition of several types of materials. However, as an R2R system can hold more than one roller, sequential deposition of multiple layers has been a main industrial application for variety of thin (or thick) film process, and can approach the quality of material deposition available through vacuum deposition processes. The thickness of deposited films is controlled accurately by the gap between the rollers, the rotational speed and the post-deposition annealing steps.

It is also possible to transfer a film grown on a metal substrate to a polymer substrate using R2R techniques. This possibility can be useful in case the deposition temperature of the functional material is beyond the operating limits for the polymeric substrate. For instance, such a transfer printing technique can be used to deposit CVD grown graphene on a polymer substrate.[70,87,89] In combination with use of inorganic nanomaterials directly deposited in a R2R process, this method is expected to save significant cost and time, compared to pure vacuum-based processes.

3 Electrically conductive species

Metal-semiconductor contacts and interconnects permit combination of devices in larger functional blocks and for us to interact with them. In general, such contacts must permit efficient conduction of charge carriers without adding to the power dissipation and losses. Traditionally, formation of such conductive layers has involved metallization using processes such as sputtering, evaporation and electron-beam deposition. While these processes are mature and well-tested, and corresponding library of metal-semiconductor combinations has been developed over the years for a variety of electronic and optoelectronic / photonic devices, these processes are not seamlessly integrated into the solution-processed de-

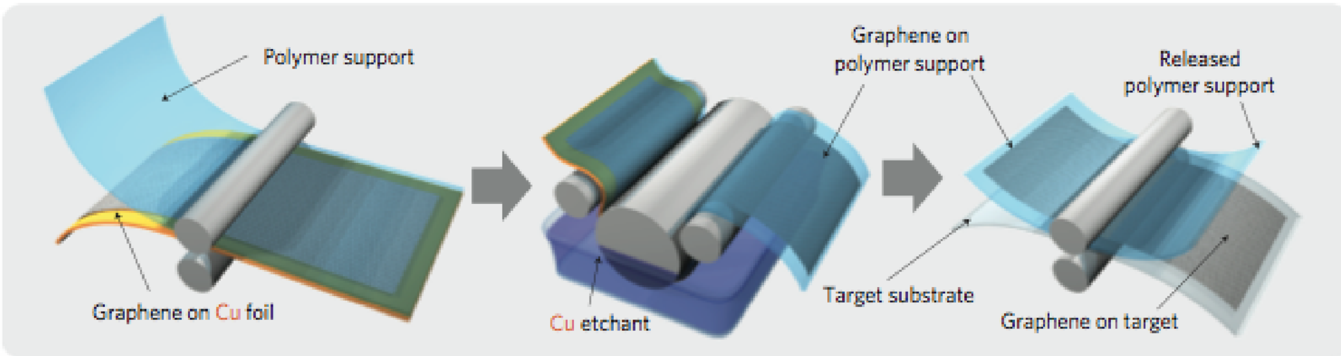

Fig. 3 Schematic of the roll-based production of graphene films grown on copper foil. Reproduced with permission.[71]

position workflow, and thus can add a significant overhead.

Over the last 10-15 years, it has been realized that besides metals, a host of different materials,[17,90–94] such as metal nanoparticles, graphene,[95] carbon-nanotubes (CNTs),[96,97], conductive polymers,[98] and transparent conductive oxides.[99] can be employed as efficient conductive layers. Formation of suitable metal nanoparticle inks depends on synthesis of nanoparticles of the correct size range for low sintering temperatures ($\sim$ 50 nm), use of surfactants to prevent their agglomeration, stabilization in solution for a reasonable shelf life (few months), high weight loading needed for sintering to result in conductively continuous films, high volatility for the functional groups / surfactants when deposited on the substrate to maximize conductivity and use of low-cost metals such as aluminium and copper, but somehow avoid oxidation and loss of conductivity (especially in the case of aluminium). Ink formulations based on metallic nanoparticles have received extensive attention in recent years and new routes of metallic nanoparticle synthesis have been developed.[100–105] Steric stabilization of colloidal nanoparticles is a standard method of stabilization in inks,[106] while use of polymeric functional groups,[107] and more recently, antioxidants,[108] has proven effective in preventing oxidation of metallic nanoparticles, especially for copper. Owing to growing indium shortage,[109,110] finding alternatives to indium tin oxide (ITO) nanoparticles or ITO substrates (for instance, sputtered ITO on XG glass has a thickness of 145 nm, transmittance of 88% at 550 nm, with a sheet resistance of approximately 20 Ω/sq.) has attracted attention. In that context, other transparent conductive materials[111,112], have assumed even greater significance. In the discussion that follows, while several different units for resistivity, conductivity and sheet resistance have been cited from recent literature, we have collected several of these results together in a consistent set of units in Table 1.

Chen *et al.*[113] have developed a new Ag nanoparticle ink formulation based on a [Ag(dien)](tmhd) complex with hexylamine and ethyl cellulose with a minimum resistivity of $\sim$ 60 $\mu\Omega$ cm at a sintering temperature of 150°C. A lower resistivity was reported by Tao *et al.*[114] who used a metallorganic ink with ethanolamine as an additive and various aldehyde-based reducing agents to produce conductive films of resistivity values between 6-9 $\mu\Omega$ cm. Shen *et al.*[107] have developed poly(acrylic acid) coated silver nanoparticles which exhibit long-term stability and a resistivity of 3.7 $\mu\Omega$ cm with a sintering temperature of 180°C. Molina-Lopez *et al.*[115] used a sintering temperature of 150°C for their comb-like printed silver contacts for a humidity sensor. Rivadeneyra *et al.*[116] used a similar structure on polyimide substrate, but with a longer sintering step at 120°C. An even lower sintering temperature ($\sim$ 100°C) was used by Jung *et al.*[117] by reducing the weight percentage of oleylamine through a ligand-exchange reaction with acetic acid. Bromberg *et al.*[118] used a plasma process (at 900W) with printed silver nitrate ink to produce a resistivity of 1.7×10^{-8} Ω m, comparable to the resistivity of bulk silver. The process had a maximal substrate temperature of 75°C, which makes it attractive as a deposition technique on low-cost substrates. Abulikemu *et al.*[119] have carried out a reactive inkjet synthesis of gold nanoparticles (size$\sim$ 8 nm) at 120°C. Nanoparticles of greater material complexity (bimetal@carbon core-shell and metal@carbon) have been synthesized using reaction under autogenic pressure at elevated temperatures (RAPET) to produce conductivities of printed lines that range from 170-4400 S/cm.[120] Kang *et al.*[30] have developed a printed nano-floating-gate memory device based on different types of metallic nanoparticles.

The use of metallic nanoparticles requires post-print sintering of the printed layers to form electrically continuous and highly conductive layers, as exemplified in the ensuing discussion. While the melting points of metals like Al, Ag, Cu and Au are much higher than the highest tolerable temperatures for most flexible substrates, sintering of nanoparticles occurs at a much lower temperature in the case of thermal sintering.

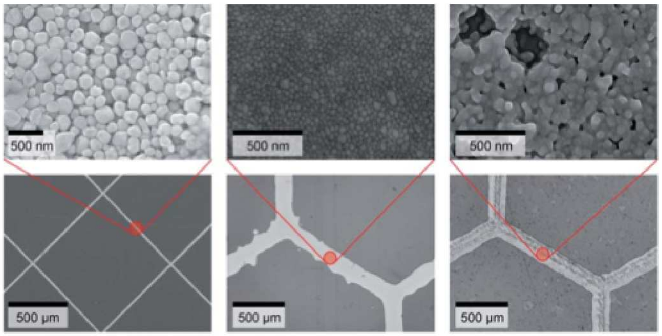

Fig. 4 SEM images for nanoparticles for three different silver electrodes and their corresponding optical images. The grid on the left is prepared using thermal imprinting, the one in the middle using inkjet printing, and the one on right using flexographic printing. Reproduced with permission.[22]

This feature can be intuitively understood as a thermodynamic effect arising from the reduction of total surface energy,[121,122]

$$\Delta(\gamma S) = S\Delta(\gamma) + \gamma\Delta(S) \quad (2)$$

where γ is the specific surface energy and S is the total surface. Since the surface to volume ratio for nanoparticles increases with decreasing particle size, the overall energy of the printed nanoparticle ink can be thought to reduce with reduction in the surface area wrought by the joining of nanoparticles. Thus, the same physics that drives the agglomeration of nanoparticles in solution, where it is undesirable, works to our advantage by reducing the sintering temperature to below the equilibrium value, namely the melting point. Insights from chemical studies of catalytic activity have further informed our understanding of the energetics of sintering.[7,123,124]The electrical and mechanical properties of sintered printed ink are particularly important for design of flexible devices with interconnects.[44,125] Several different types of sintering methods are in use - thermal,[126] photonic,[127,128] plasma/electrical,[129,130] and microwave.[131,132] While the reader is referred to comparative studies on this subject,[133] some recent reports involving two-step sintering,[134,135], consideration of laser-induced temperature field in laser sintering[136] and a potential approach to room-temperature sintering of silver nanoparticles,[137] represent further progress in the development of high conductivity, low-temperature, defect-free metallic lines on flexible substrates. An alternative approach to forming low-temperature conductive films was demonstrated through formation of a network of nearly transparent coffee-rings obtained from inkjet printing.[138] UV-curing was used in the room temperature sintering of silver nanoparticles as a yet another approach.[139] The surface morphology (Fig. (4)) of the printed electrodes is expected to play an important role in the performance of devices with printed electrodes. Grain size optimization and prevention of too many dead spots is likely to yield better device performance.

3.1 Alternative conductive materials

The aforementioned challenging requirements for metallic nanoparticles have prompted researchers to consider alternatives to metallic nanoparticles, such as CNTs and graphene.[140,141] The high aspect ratio of CNTs coupled with van der Waals interactions between them usually lead formation of *bunches* of CNTs and eventual clogging of printheads.[96] A very similar effect occurs in the case of graphene solutions, whereby an inter-flake interaction between exfoliated graphene flakes leads to formation of *sandwiches* of graphene, which in turn makes it necessary to functionalize graphene to reduce such interactions.[142,143] Recent work on non-covalent functionalization of graphene has increased the prospects of high weight loading of graphene inks.[144]

Transparent conducting oxides and hybrid materials based on them are yet another set of promising materials for conductive layers, especially for solar cells.[145–148] Doped binary and ternary oxides permit a fine tuning of resistivity and toxicity.[111] Alternatives to conductive oxides include graphene based materials as discussed above. Wang *et al.*[57] used a printable aqueous graphene oxide (GO) ink using a non-ionic surfactant. When coated on a flexible glass, and subjected to a 650°C anneal, the reduced graphene oxide (RGO) film showed a transmittance of 45% at 550 nm and a sheet resistance of 5370 Ω/sq.

Xu *et al.*[149] have inkjet printed a composite nano graphene platelet (NGP)/polyaniline (PANI) ink to produce layers with conductivity of 3.67 S/cm for supercapacitors with energy density of 2.4 Wh/kg. Chen *et al.*[150] have screen-printed a composite layer consisting of Al nanoparticles and wrinkle-like graphene sheets to achieve a 7.2% enhancement in the photocurrent of a silicon solar cell. Giardi *et al.*[151] have used a graphene oxide (GO) / acrylic (poly(ethylene glycol)) composite ink in conjunction with UV-curing to demonstrate a non-thermal route. The thermal reduction of GO represents an increasingly popular deposition route for graphene.[152] Secor *et al.*[153] directly printed solution-phase exfoliated graphene to obtain a resistivity of 4 mΩ cm after a 250°C anneal for 30 min. Much higher conductivities ($\sim$ 420 S/cm) were achieved by Su *et al.*[154] with weakly oxidized GO and used in a single-wall CNT FET exhibiting a mobility of 8cm$^2/(V \cdot s)$. Organic field-effect transistor (OFET) performance enhancement with the use of GO on a silicon oxide substrate with triisopropylsilylethynyl (TIPS) pentacene[155] with printed silver drain and source contacts has recently been reported and attributed to enhanced grain size.

Table 1 Summary of some recent results of deposition of conductive species. Method=deposition method. Other columns: d= Particle size (nm), ρ=Resistivity ($\mu\Omega\cdot$ cm) reported in the study, C% = Maximal percentage of the bulk conductivity achieved in the study (=$\frac{\rho_{bulk}}{\rho}\times 100$), T% = Transparency. Some abbreviations: IJP=Inkjet Printed. SP=Screen Printed. BP=Brush-painted. D=Dispensed. DB = doctor bladed. MOD = Metallorganic Decomposition. UV = Ultraviolet. GO=Graphene Oxide. RGO=Reduced Graphene Oxide. WGO=Weakly oxidized Graphene Oxide. NGP=Nano Graphene Platelets. NW = nanowires. Curing conditions involve thermal sintering/annealing unless indicated otherwise. Starred numbers (and columns) have been calculated from provided data.

Method	Material/ref.	d (nm)	Ink chemistry	Curing	$\rho(\mu\Omega\cdot$cm)	C%*	T%
IJP	Ag [138]	5-20	poly(acrylic) acid / Byk-348 / amino methyl propanol	30	43(120* for 2D)	4	95
IJP	Ag [35]	2-3	Tetradcane	130°C	<25	> 6	-
Thermal imprint/IJP	Ag [22]	216/45	Water/-	140/140°C	25/1200*	6.36 / 0.1	82/71
IJP	Ag [116]	< 150	Ethanol	150-300 °C	21-25	8	-
SP	Ag NW [156]	25700×187	Ethanol	Compaction	16.47*	9.65	-
IJP	Ag(MOD) [139]	-	-	UV	15.39*	10.33	-
IJP	Ag [128]	30-50	poly (vinylpyrrolidone) / ethylene glycol / ethanol / glycerol	Photonic flash sintering	14.31*	$\frac{100}{9}$	-
D	Ag [136]	518 × 30	Ethanol	200	7.4	21.5	-
IJP	Ag [137]	11.1	poly(acrylic acid) sodium / poly (diallyldimethylammonium chloride)	Chemical sintering	6.8	23.4	-
IJP	Ag [114]	< 100	Ethanolamine	90-120°C	6-9	27	-
IJP	Ag [113]	<20	Hexylamine / Ethyl cellulose	250°C	4.625-9.376	34.378	-
IJP	Ag [117]	12.2	Ethanol	150-250 °C	4.54-7.13	35.02	-
IJP	Ag [37]	50	-	Laser	4.07	39.1	-
IJP	Ag [107]	40	Water / Monoethanolamine	50-180°C	3.7-139	43.0	-
IJP	Ag [130]	10-20	Triethylene glycol monoethyl ether	Electrical sintering	2.7*	58.9	-
IJP	Ag [118]	-	$AgNO_3$/Water	Plasma	1.7	93.5	-
IJP / DB	Ag / PEDOT:PSS [134]	-	Isopropyl alcohol	65°C / 225°C	170*	1	-
BP	Ag NW / ITO [157]	See ref.	-	ITO:100°C / Ag: 150 °C	1090	-	79.50
EHD / BP	Ag / ITO [158]	10-25	Ethanol	200°C	42	-	83.72
BP	$Ti:In_2O_3$ [159]	20-40	Ethanol	350-500°C	∼ 3000	-	85.48
IJP	Cu@Ag@C/ Ag@Cu@C [120]	50	Water / ethylene glycol (butyl or methyl) ether / isopropanol / Byk-Jet 9132	-	227.3 - 5882.4*	-	-
Meyer Rod	RGO [57]	-	Water / Zynol	650°C	13425*	-	45
IJP	GO [151]	-	Water / poly(ethylene glycol) diacrylate	UV	$\sim 3\times 10^{12}$	-	-
IJP	WGO [154]	-	Ethylene glycol / Na dodecylbenzenesulfonate	100°C	2381*	-	-
IJP	Graphene [153]	-	Ethyl cellulose / cyclohexanone / terpineol	250°C	4000	-	-
IJP	NGP/PANI [149]	40-80	PANI / surfactant / water	80 °C	2.72×10^{6}*	-	-
IJP	$SWCNT/RuO_2$ NW [160]	-	Water/Na dodecyl sulfonate	-	625*	-	10-80

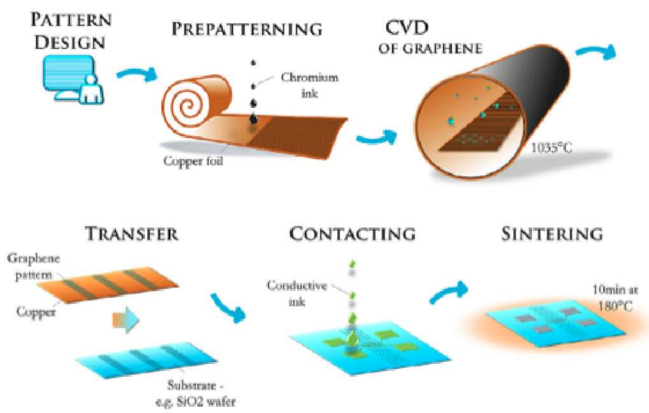

Fig. 5 A process employing inkjet print patterning, deposition and pattern transfer to produce graphene FETs. Reproduced with permission.[163]

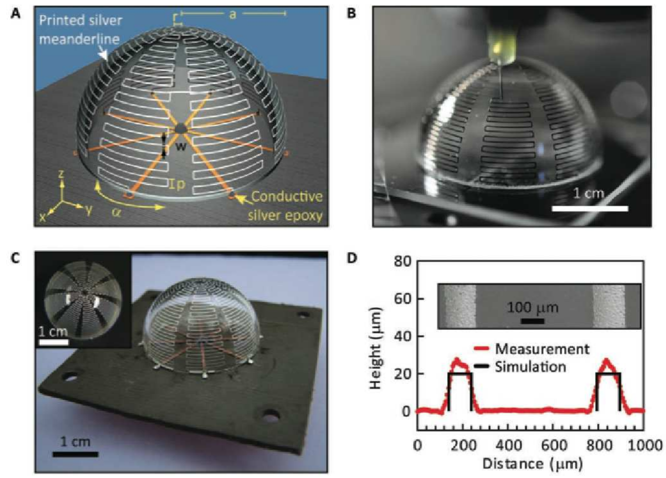

Fig. 6 Conformal direct printing of an electrically small antenna, with optical images and optical profileometry results. Reproduced with permission.[169]

The use of different nanomaterial systems together in the same device, either as separate components, or as hybrid materials has found applications in recent years. Xie *et al.*[161] used inkjet printed silver contacts and spray coated functionalized multi-wall CNTs (MWCNTs) to demonstrate a humidity sensor on paper. Jeong *et al.*[158] have used an invisible silver grid in combination with an ITO nanoparticle layer as a transparent contact. They also have demonstrated a variant with silver nanowires,[157] and titanium-doped indium oxide,[159] with brush painting. The high surface to volume ratio of CNTs (with RuO_2 nanowires) has found applications in flexible supercapacitors[160] and in electrothermal applications involving effective Joule heating (with graphene-based materials).[162] Hurch *et al.*[163] have used inkjet printing in two different ways to pattern a channel for chemical vapor deposited (CVD) graphene and the conductive contacts while transferring the print-defined pattern from a copper foil to a different substrate. This hybrid process is exhibited in Fig. (5). Transfer techniques have also been used for n-OFETs with gold electrodes[164] to reduce the inverse subthreshold slope and increase linear region mobility by 200%, a performance comparable to low-work function materials like Al and Ca (which are unstable in air).[165]

3.2 Low-cost substrates

Low cost substrates like paper using pulp and nanofibrillated fibers have attracted attention as alternative flexible substrates. A recent comparative study[166] using sputtered gold, silver nanoparticle ink and particle-free metallorganic silver ink have yielded very low resistivities. In another report,[167] a recyclable paper substrate was also used to fabricate an electrochemical analysis platform using printed gold for working and counter electrode, while a printed silver stripe formed the basis of the reference electrode. Huang *et al.*[156] have developed a printing-filtration-press (PFP) technique for mass production of flexible bending-resistant paper-based circuits with a conductivity of ∼ 61,000 S/cm, using silver nanowires. They have demonstrated this technique for radio frequency identification (RFID) tags and cellphone cables. Inkjet printed antenna structures on a variety of substrates and in a variety of shapes, using direct and catalyst printing[27,168–170] have been demonstrated. Using a variety of conductive nanomaterials discussed above, given the wide applicability of RFID-based devices,[171,172] there have been reports of printed RFID-based sensors[173,174], gas sensors,[175,176], biomedical sensor nodes,[177], hemispherical antennas (Fig. (6)),[169] and microfluidic RFID-enabled platforms for wireless lab-on-chip applications.[178] Paper-based bio-sensors have found a special niche as disposable, low-cost and portable sensors for protein analysis, lab-on-chip applications, and environmental toxins.[179] Shemelya *et al.*[180] used copper wires as a capacitive sensor embedded in printed polycarbonate with sensitivity better than 0.1%. Cheap force sensors can be also be fabricated using printing methods.[181]

With the use of low-cost substrates like plastic and paper, and other flexible substrates, it is also important to consider the mechanical stability of the devices, in response to flexion and bending. Repeated stress can lead to strain in various layers, delamination and device failure. Studies that test for stability towards repeated strain are thus essential before commercialization of any flexible devices.[182–184]

4 Semiconducting, and insulating species

While conductive layers can be inorganic, such as for transparent conductive oxides, in this section, we briefly survey the current state of art in printing of inorganic nanoparticles as functional components of different electronic and interestingly, non-electronic devices. Inorganic nanoparticles, find offer prospects for or current applications in quantum-dot based light-emitting diodes (QDLEDs),[185–187], organic-inorganic hybrid material based LEDs[188,189], solar cells,[190–192], gas sensors,[193], photovoltaics.[194–196] and biosensors.[197] We have briefly discussed sintering of nanoparticles in Sec. (3). In the discussion that follows, it is implicitly assumed that sintering of inorganic nanoparticles[91,198] is governed by similar physics.

There has been a resurgence in research interest in dye-sensitized solar cells due to advances in materials, material deposition methods, and solid phase electrolytes. Screen printed[190,191,199–202] and inkjet printed[199,203] TiO_2 nanoparticles and other nanosystems like titanium oxide nanobundles[204] are common photoelectrodes for organic and dye-sensitized solar cells. Conventional room temperature methods of forming TiO_2 paste involve suspending the nanopowder in ethanol, sonication and adding titanium tetraisopropoxide (TTIP) as a hydrolyzing agent to form a stable and uniform suspension.[205] Recently, Dar *et al.*[206] demonstrated a microwave-based approach to synthesize anatase titania nanomaterials in two different size regimes for functionally different parts of a dye-sensitized solar cell exhibiting efficiency of 6.5%. Titania nanomaterials can be deposited using nanomaterials of different dimensionality and size using screen printing.[207] Chang *et al.*[208] doped TiO_2 with up-converting nanoparticles to form $TiO_2/NaYF_4:Yb^{3+}$, Er^{3+} nano-heterostructures, which were fabricated using screen printing of the resulting paste. They found that the samples with the up-converting nanoparticles showed a 17% improvement over samples that did not. Other reported methods of increasing efficiency of the photoanodes in solar cells involve tungsten doping.[209]

Besides titanium oxide, other viable species such as ZnO[192,210] and $BiVO_4$[211] have also attracted interest over recent years. Kwon *et al.*[212] showed direct selective growth of ZnO nanowires using a zinc acetate ink precursor, and demonstrated field-effect transistors and UV photodetectors using this fabrication method. Printing of composite ZnO-TiO_2 nanoparticles and screen printing of TiO_2 paste on to ZnO microrod arrays grown on glass[213] are methods of producing a complex nanocomposite. In-situ growth of MgO and ZnO films through printing of acetate solutions,[214] and self-organized growth of CuO hollow spheres are examples of alternative to pre-synthesis and subsequent deposition.[215] Other possible composite components include graphene[216] which have been used to fabricate dye-sensitized solar cells. Krebs *et al.*[82] have demonstrated a complete R2R process involving ZnO nanoparticles (Fig. (7)).

Chalcogenide material systems have attracted significant interest due to the wide variety of n- and p- type materials available with differing mobilities, and synthetic methods for large scale production of nanoparticles have been developed.[217] More complicated nanomaterial systems[218] can be created with in-situ growth of PbS nanoparticles on ZnO nanowires using a printing-based approach. Bronstein *et al.*[219] have used CdSe/CdS seeded nanorods as a tunable lumophore with embedded, transfer-printed crystalline Si solar cells. The resulting area of the luminescent concentrators is 5000 times the area of the solar cell. Nguyen *et al.*[220] have printed (using a doctor blade method) Cu(In,Ga)S_2 nanoparticles and selenized to form Cu(In,Ga)Se_2 (CIGS) solar cells. After annealing and etching with KCN, they found improved photovoltaic performance. Application of rapid thermal processing methods[221] can help speed up the fabrication of CIGS solar cells even further.

Boulfrad *et al.*[222] have used perovskite-based nanomaterials to demonstrate scalable anodes for solid oxide fuel and electrolysis cells. They doped x% wt. $Ce_{0.9}Gd_{0.1}O_{2-\delta}$ (CGO) into $(La_{0.75}Sr_{0.25})_{0.97}Cr_{0.5}Mn_{0.5}O_3$ (LSCM) and coated it with y% nickel oxide or nickel nitrate to prepare a screen printable ink in an organic solvent for the anode. An ink comprised of $(La_{0.8}Sr_{0.2})_{0.95}MnO_3$ (LSM) was prepared for the cathode. Three compositions - A(x=15,y=0), B(x=15,y=5,source=NiO) and C(x=15, y=5, source=Ni$(NO_3)_3$) were tested. The results of impedance measurements carried out at two different temperatures, with a fuel source: H_2 + 3% water vapor are shown in Fig. (8).

Piezoelectrics like lead zirconate titanate (PZT) form the basis of functional layers involving interplay of mechanical movement and charge state, and advances in synthesis of suitable inks[223,224] and printing processes[225] are significant.Wei *et al.*[226] reported the design, fabrication and testing of a planar valveless micropump screen printed on to a polyimide substrate. They achieved a maximum flow rate of 38 μl/min using a drive frequency of 3 kHz.

While organic and polymeric species have found applications as diverse as OLEDs,[227–230] piezoelectric actuators,[231] ferroelectric memories,[232] pioneering work on reinforced composites employing thermoplastic polymers,[233,234] and solar cells,[19,235–238] the printing of polymer- and organic semiconductor based nanoparticles has revealed them to be functional materials with several applications. To promote adhesion of polymer species on common substrates, variants of printing processes like polymer grafting[239] have been developed. Interestingly, inkjet printing of molten precursors has been used to produce polymers like nylon 6.[240] Being soft materials, polymer nanoparticles are suspect to a change in their

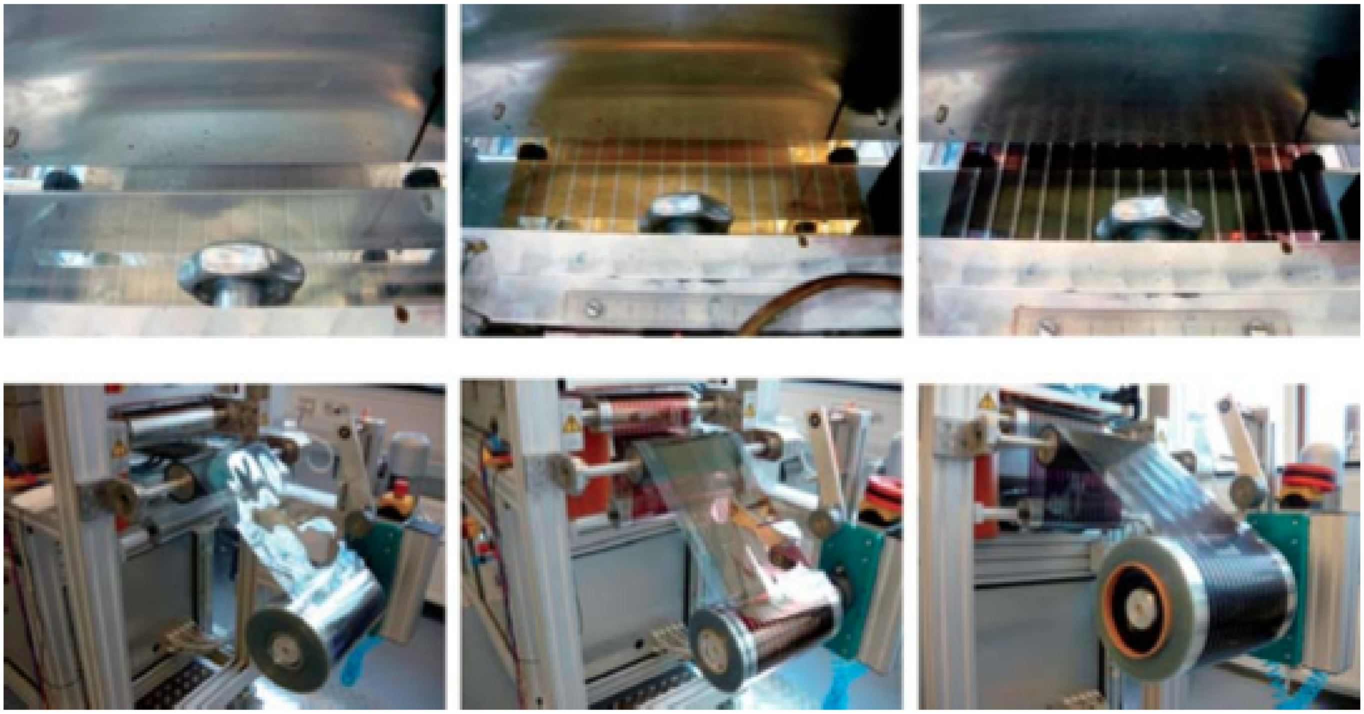

Fig. 7 The slot-die coating of ZnO nanoparticles (left), P3HT:PCBM (middle) and PEDOT:PSS (right). Wet films on the top, dried ones are shown below.Reproduced with permission.[82]

properties in response to mechanical stress.[241] Given the presence of conjugated carbon-carbon bonds, it is not surprising that many polymer nanomaterial systems are good potential candidates for biosensing applications. Weng *et al.*[242] have demonstrated a fully-printed polypyrrole (PPy)-based biosensor consisting of inkjet printed biomaterials composed of PPy-enzyme formulations on to screen printed carbon electrodes. They found a peroxide detection threshold value of 10μM and a higher threshold for glucose, 1mM. Hibbard *et al.*[243] have used printed polyaniline(PANI) nanoparticles to create an ammonia sensor for human breath. Several other sensor applications involving PANI have been reported and reviewed.[244] Eissa *et al.*[245] have used microcontact printing to deposit epoxy-functionalized magnetic colloidal particles for specific antigen detection.Akagi *et al.*[246] have used inkjet printing of layer-by-layer poly(lactide) stereocomplex as a drug vector with up to 100% wt. loading. Citterio group[247] have created an inkjet printed colorimetric sensor array for discrimination of volatile primary amines through sensitivity to polarity of the species. Tang and Feng[248] have reviewed conjugated polymer luminescent nanoparticles for imaging and therapeutic applications.

5 Biological and pharmaceutical species

Biological tissue differs in essential ways from materials discussed so far. The chemical composition largely consists of the elements of life - C, H, N, O, P and S, in addition to elements like Ca which form the bulk of bone tissue, in two major components organic collagen and inorganic hydroxyapatite ($Ca_{10}(PO_4)_6(OH)_2$). Bone growth occurs as a result of mineralization involving osteoblasts, which are bone-forming cells within the human body. Due to wasting diseases like polio or traumatic loss of bone tissue, it sometimes becomes necessary to replace bone tissue. While the subject of bone implants and reconstruction is beyond the scope of this review, it should be noted that the use of nanomaterials has been known to enhance *in vitro* and *in vivo* osteoblast function, which indicates that the process of integration of implants (osseointegration) is augmented by the use of nanostructured metals, ceramics, polymers and composites.[249]

Thus, it should not be surprising that the first attempts to employ printing (especially 3D printing) in biotechnology involved bone tissue engineering (BTE). Powder-based nanomaterials like calcium phosphates[250] have been used for their superior biocompatibility and mechanical strength.[44,251–255] 3D printing has been used to fabricate scaffolds,[256–258] followed by their installation on to damaged bone. During this

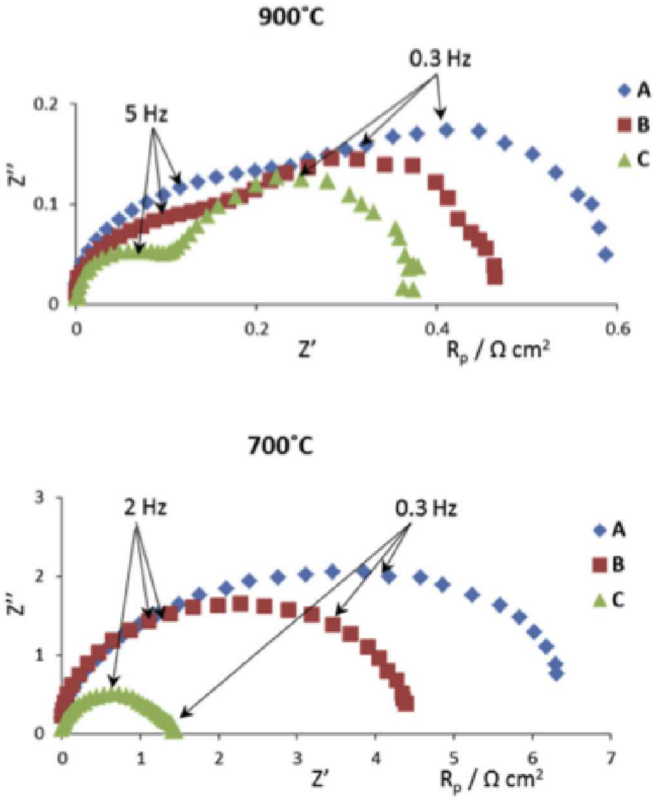

Fig. 8 Impedance diagrams for three different anode compositions under 50 ml/min pure wet hydrogen gas flow. Reproduced with permission. [222]

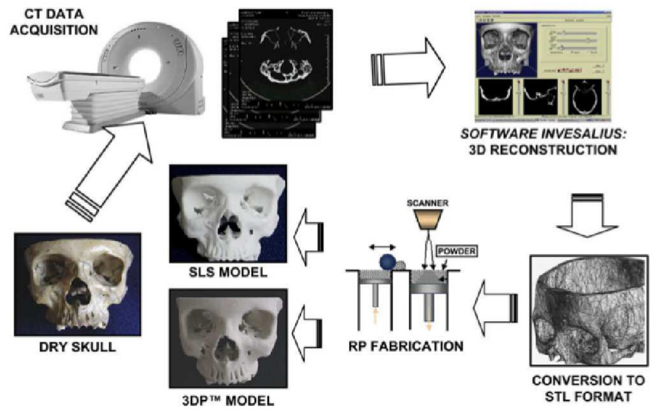

Fig. 9 Steps involved in prototyping a human skull using 3D printing methods (selective laser sintering). Reproduced with permission. [266]

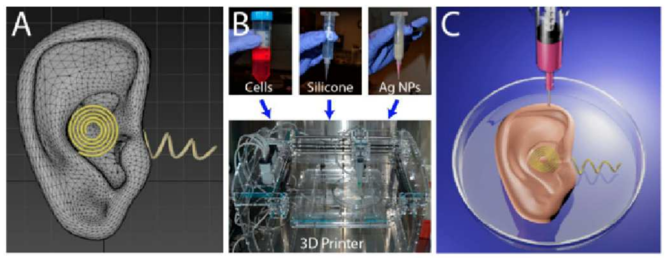

Fig. 10 Three-dimensional interweaving of biology and electronics via additive processes. Functional materials used include chondrocytes, silicone and silver nanoparticle ink fused silicone. Reproduced with permission. [267]

process, polymers are used to bind calcium phosphate powder and then heat treated to form a permanent connection after the print. [259–262] The organic component of natural bone tissue, collagen, has also been used in 3D printing. [263–265] Besides being bone replacement tissue, 3D printing is also critical to fabrication of biomedical prototypes as a diagnostic aid or for planning of bone / tissue surgery as shown in Fig. (9).

As is evident from the cited work above, most of the work involving 3D printing has been focused on the design of bone scaffolds as they serve as a three-dimensional template for initial cell growth. [44,254] However, a scaffold must have a highly porous structure [257,258] that permits cell migration and nutrition. A pore size suitable for this purpose is estimated to be in the range of 50-1000 μm for effective bone regeneration. [260]

Three-dimensional networks consisting of hydrophilic polymer chains with high water content, or hydrogels, [269] have been deposited using printing, especially for bionic organs and cybernetics. [270–275] Fig. (10) shows a functional bionic ear that is mechanically and acoustically similar to a human ear. [267] There have been reports of hydrogel synthesis from natural

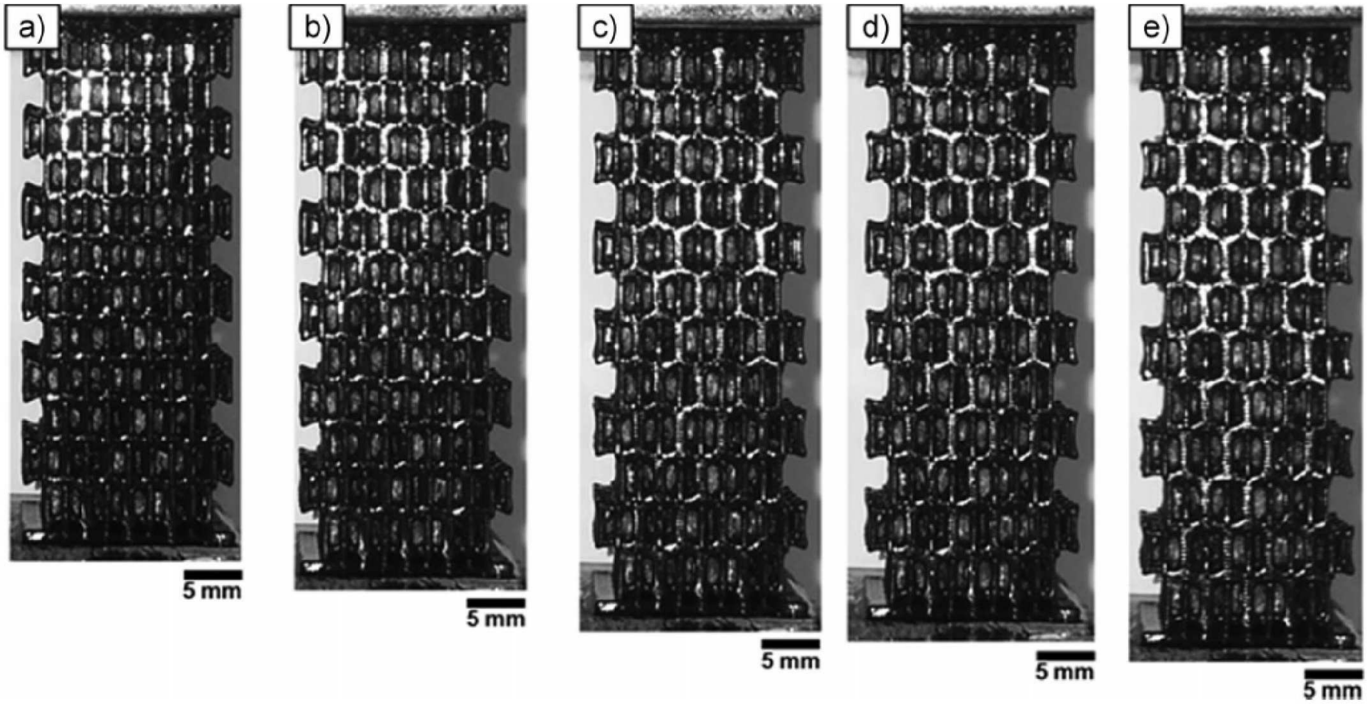

Fig. 11 Sequence of strain induced structural changes in a 3D printed auxetic foam from (a) re-entrant lattice to (e) honeycomb structure. The strains are as follows; (a) 0%, (b) 5%, (c) 12%, (d) 14%, and (e) 19%. Reproduced with permission.[268]

and synthetic sources and used for drug delivery, stem cells, and cancer research.[276–281] Due to the mechanical limitations of natural hydrogels such as collagen, chitosan, hyaluronic acid (HA), gelatin, elastin, etc., these have been replaced by synthetic hydrogels such as poly(ethylene glycol) (PEG), poly(vinyl alcohol)(PVA), and poly(acrylamide)(PAM) in several recent studies.[54,260] These hydrogels have been used as an artificial extracellular matrix supporting regeneration of various tissues. Hydrogels can be freely printed as they do not generally give rise to nozzle clogging.[282]

Auxetic structures (Fig. (11))[268] occur naturally in cubic elemental metals, α-cristobalite, biological tissues (for instance, in feline skin). Polyurethane foams exhibit a similar behaviour with tri-axial volumetric compression and relaxation. Such a structure can be replicated using 3D printing methods and used in creation of complex structures with emergent properties, such as metamaterials for a suitable wavelength.

6 Conclusions

We started this review article with a discussion of additive processes and nanomaterial systems with an argument that the class of processes and the class of materials were well suited to be combined to fabricate new kinds of devices with performance that is not achievable with conventional subtractive processes acting upon bulk materials. While not exhaustive, in this review, we have attempted to provide a fairly wide-ranging and nearly feature-complete view of the field. It is quite apparent that for several classes of devices, the performance difference between the vacuum deposition and the solution-processed printed version is beginning to shrink or even disappear altogether.

Already, subtractively fabricated nanosystems under vacuum provide very high efficiency solar cells (III-V multi-junction concentrators), and very short channel FETs with acceptable transfer characteristics, three-dimensional gated structures, etc. However, the dimensional limits of subtractive processes are now beginning to show themselves. For the first time in over four decades, Moore's law is no longer expected to double the number of transistors on a chip every 18 months. Such a situation suggests quite naturally the fabrication of devices starting from the other length extreme - atoms and molecules.

However, nanomaterials possess a high surface to volume ratio, which results in a stronger coupling between material properties and processing parameters, such as solutions, impurities in the ambient, and interaction with other nanomaterials. While the latter interaction is often physically desirable in design of materials with emergent properties, unintentional or unforeseen interactions modify the physical behaviour of these nanosystems in unpredictable ways and are responsible for some of the performance degradation seen in non-vacuum processes. While the removal of all unintentional chemistry at the nanoscale is not possible for solution-processes, the active addition of chemistry, in the form of functionalized nanoparticles that are more stable in solution than bare nanoparticles, suggests itself to be one possible route forward.

It will be interesting to see the effect of applying biological principles and self-assembly to create new material properties, while combining nanoscale chemistry with a combination of many different printing processes to access different length scales of material organization. A tantalizing possibility that exists involves the use of purely a synthetic approach coupled with printing processes to achieve all device architectures currently accessible through expensive, low-throughput methods of device fabrication, such as e-beam lithography, focussed ion beam, atomic layer deposition, etc. For purposes of future nanoscale devices that meet our ever more demanding specifications, it is essential that this possibility be met to achieve the necessary industrial scale-up.

References

1 S. A. Campbell, *The science and engineering of microelectronic fabrication*, Oxford University Press, 2nd ed edn., 2001.

2 R. G. Hobbs, N. Petkov and J. D. Holmes, *Chemistry of Materials*, 2012, **24**, 1975–1991.

3 M. Shimomura and T. Sawadaishi, *Current Opinion in Colloid & Interface Science*, 2001, **6**, 11–16.

4 N. C. Seeman and A. M. Belcher, *Proceedings of the National Academy of Sciences*, 2002, **99**, 6451–6455.

5 W. Lu and C. M. Lieber, *Nature Materials*, 2007, **6**, 841–850.

6 J. Willmann, D. Stocker and E. Dörsam, *Organic Electronics*, 2014, **15**, 1631–1640.

7 T. A. Campbell and O. S. Ivanova, *Nano Today*, 2013, **8**, 119–120.

8 H. J. Gysling, *Current Opinion in Colloid & Interface Science*, 2014, **19**, 155–162.

9 M. Singh, V. Ranjan and V. A. Singh, *International Journal of Modern Physics B*, 2000, **14**, 1753–1765.

10 A. M. Elliott, O. S. Ivanova, C. B. Williams and T. A. Campbell, *Advanced Engineering Materials*, 2013, **15**, 903–907.

11 P. Wang, J. Ma, F. Shi, Y. Ma, Z. Wang and X. Zhao, *Industrial & Engineering Chemistry Research*, 2013, **52**, 10355–10363.

12 F. Zhu, N. P. Macdonald, J. M. Cooper and D. Wlodkowic, *Micro/Nano Materials, Devices, and Systems*, 2013, **8923**, 892344–892344–14.

13 O. Ivanova, C. Williams and T. Campbell, *Rapid Prototyping Journal*, 2013, **19**, 353–364.

14 M. Singh, H. M. Haverinen, P. Dhagat and G. E. Jabbour, *Advanced Materials*, 2010, **22**, 673–685.

15 J. G. Korvink, P. J. Smith and D.-Y. Shin, *Inkjet-based Micromanufacturing*, John Wiley & Sons, 2012.

16 P. J. Smith and A. Morrin, *Journal of Materials Chemistry*, 2012, **22**, 10965–10970.

17 A. Kamyshny and S. Magdassi, *Small*, 2014, n/a–n/a.

18 H.-W. Lin, C.-P. Chang, W.-H. Hwu and M.-D. Ger, *Journal of Materials Processing Technology*, 2008, **197**, 284–291.

19 F. C. Krebs, *Solar Energy Materials and Solar Cells*, 2009, **93**, 394–412.

20 D.-Y. Shin, M. Jung and S. Chun, *Journal of Materials Chemistry*, 2012, **22**, 11755–11764.

21 J. G. Ok, H. S. Youn, M. K. Kwak, K.-T. Lee, Y. J. Shin, L. J. Guo, A. Greenwald and Y. Liu, *Applied Physics Letters*, 2012, **101**, 223102.

22 J.-S. Yu, I. Kim, J.-S. Kim, J. Jo, T. T. Larsen-Olsen, R. R. Søndergaard, M. Hösel, D. Angmo, M. Jørgensen and F. C. Krebs, *Nanoscale*, 2012, **4**, 6032–6040.

23 R. R. Søndergaard, M. Hösel and F. C. Krebs, *Journal of Polymer Science Part B: Polymer Physics*, 2013, **51**, 16–34.

24 M. Wessling, L. G. Morcillo and S. Abdu, *Scientific Reports*, 2014, **4**, 4294.

25 X. Wang, P. Lu, N. Dai, C. Liao, Y. Wang, Q. Zheng, X. Guo and Q. Zhang, *Journal of Micromechanics and Microengineering*, 2007, **17**, 1307.

26 A. Piqué, R. C. Y. Auyeung, H. Kim, K. M. Metkus and S. A. Mathews, *JLMN - Journal of Laser Micro/Nanoengineering*, 2008, **3**, 163–169.

27 M. Singh, H. M. Haverinen, Y. Yoshioka and G. E. Jabbour, in *Active Electronics*, ed. I. M. Hutchings and G. Martin, John Wiley & Sons, Ltd, 2012, pp. 207–235.

28 R. D. Deegan, O. Bakajin, T. F. Dupont, G. Huber, S. R. Nagel and T. A. Witten, *Nature*, 1997, **389**, 827–829.

29 D. Pesach and A. Marmur, *Langmuir*, 1987, **3**, 519–524.

30 M. Kang, K.-J. Baeg, D. Khim, Y.-Y. Noh and D.-Y. Kim, *Advanced Functional Materials*, 2013, **23**, 3503–3512.

31 J.-Y. Lee, B. Choi, B. Wu and M. Lee, *Biofabrication*, 2013, **5**, 045003.

32 H. Y. Park, B. J. Kang, D. Lee and J. H. Oh, *Thin Solid Films*, 2013, **546**, 162–166.

33 J. Lessing, A. C. Glavan, S. B. Walker, C. Keplinger, J. A. Lewis and G. M. Whitesides, *Advanced Materials*, 2014, n/a–n/a.

34 H. Meier, U. LÃffelmann, D. Mager, P. J. Smith and J. G. Korvink, *physica status solidi (a)*, 2009, **206**, 1626–1630.

35 J.-U. Park, M. Hardy, S. J. Kang, K. Barton, K. Adair, D. k. Mukhopadhyay, C. Y. Lee, M. S. Strano, A. G. Alleyne, J. G. Georgiadis, P. M. Ferreira and J. A. Rogers, *Nature Materials*, 2007, **6**, 782–789.

36 T. Sekitani, Y. Noguchi, U. Zschieschang, H. Klauk and T. Someya, *Proceedings of the National Academy of Sciences*, 2008, **105**, 4976–4980.

37 D. G. Lee, D. K. Kim, Y. J. Moon and S.-J. Moon, *Nanotechnology*, 2013, **24**, 265702.

38 S. J. P. Kress, P. Richner, S. V. Jayanti, P. Galliker, D. K. Kim, D. Poulikakos and D. J. Norris, *Nano Letters*, 2014.

39 D. Engstrom, B. Porter, M. Pacios and H. Bhaskaran, *Journal of Materials Research*, 2014, **29**, 1792–1816.

40 H. K. Choi, J.-U. Park, O. O. Park, P. M. Ferreira, J. G. Georgiadis and J. A. Rogers, *Applied Physics Letters*, 2008, **92**, 123109.

41 K. Rahman, K. Ali, N. M. Muhammad, M.-t. Hyun and K.-h. Choi, *Applied Physics A*, 2013, **111**, 593–600.

42 Y. Han, C. Wei and J. Dong, *Manufacturing Letters*, 2014, **2**, 96–99.

43 P. Huang, D. Deng and Y. Chen, author, 2013.

44 I. Lee, W.-K. Oh and J. Jang, *Journal of Hazardous Materials*, 2013, **252–253**, 186–191.

45 L. Shaw and Z. Bao, *Israel Journal of Chemistry*, 2014, n/a–n/a.

46 P. G. Jessop, *Green Chemistry*, 2011, **13**, 1391–1398.

47 L. Moity, V. Molinier, A. Benazzouz, R. Barone, P. Marion and J.-M. Aubry, *Green Chemistry*, 2013, **16**, 146–160.

48 T. M. Eggenhuisen, M. J. Coenen, T. W. Slaats, H. Gorter, J. Sweelssen and P. Groen, *NIP & Digital Fabrication Conference*, 2013, **2013**, 203–205.

49 G.-H. Lim, J.-M. Zhuo, L.-Y. Wong, S.-J. Chua, L.-L. Chua and P. K. H. Ho, *Organic Electronics*, 2014, **15**, 449–460.

50 C. Hull, *Apparatus for production of three-dimensional objects by stereolithography*, Google Patents, 1986.

51 D. Velenis, M. Stucchi, E. Marinissen, B. Swinnen and E. Beyne, IEEE International Conference on 3D System Integration, 2009. 3DIC 2009,

2009, pp. 1–5.
52 B. C. Gross, J. L. Erkal, S. Y. Lockwood, C. Chen and D. M. Spence, *Analytical Chemistry*, 2014, **86**, 3240–3253.
53 M. Eisenberg, *International Journal of Child-Computer Interaction*, 2013, **1**, 7–13.
54 P. Zorlutuna, N. Annabi, G. Camci-Unal, M. Nikkhah, J. M. Cha, J. W. Nichol, A. Manbachi, H. Bae, S. Chen and A. Khademhosseini, *Advanced Materials*, 2012, **24**, 1782–1804.
55 H. Kang, J. Lee, S. Jung, K. Yu, S. Kwon, S. Hong, S. Kee, S. Lee, D. Kim and K. Lee, *Nanoscale*, 2013, **5**, 11587–11591.
56 D. Zopes, R. von Hagen, R. Müller, R. Fiz and S. Mathur, *Nanoscale*, 2010, **2**, 2091.
57 J. Wang, Z. Fang, H. Zhu, B. Gao, S. Garner, P. Cimo, Z. Barcikowski, A. Mignerey and L. Hu, *Thin Solid Films*, 2014, **556**, 13–17.
58 Y. Zhang and J. R. G. Evans, *Journal of Colloid and Interface Science*, 2013, **395**, 11–17.
59 C. Polzin, S. Spath and H. Seitz, *Rapid Prototyping Journal*, 2013, **19**, 37–43.
60 W. D. Teng, M. J. Edirisinghe and J. R. G. Evans, *Journal of the American Ceramic Society*, 1997, **80**, 486–494.
61 M. Mott, J.-H. Song and J. R. G. Evans, *Journal of the American Ceramic Society*, 1999, **82**, 1653–1658.
62 K. A. M. Seerden, N. Reis, J. R. G. Evans, P. S. Grant, J. W. Halloran and B. Derby, *Journal of the American Ceramic Society*, 2001, **84**, 2514–2520.
63 X. Zhao, J. R. G. Evans, M. J. Edirisinghe and J.-H. Song, *Journal of the American Ceramic Society*, 2002, **85**, 2113–2115.
64 J. Hiller and H. Lipson, *Rapid Prototyping Journal*, 2009, **15**, 137–149.
65 W. Wang, T. Y. Wang, Z. Yang, L. Liu, X. Tong, W. Tong, J. Deng, F. Chen and X. Liu, *ACM Trans. Graph.*, 2013, **32**, 177:1–177:10.
66 Z. Kappassov, Y. Khassanov, A. Saudabayev, A. Shintemirov and H. Varol, 2013 IEEE International Conference on Mechatronics and Automation (ICMA), 2013, pp. 1697–1702.
67 J. Gonzalez-Gomez, A. Valero-Gomez, A. Prieto-Moreno and M. Abderrahim, in *A New Open Source 3D-Printable Mobile Robotic Platform for Education*, ed. U. Rückert, S. Joaquin and W. Felix, Springer Berlin Heidelberg, 2012, pp. 49–62.
68 J. Robinson, *Expiring patents were supposed to boost the 3D printing market. They haven't*, 2014, `http://pando.com/2014/06/06/expiring-patents-were-supposed-to-boost-the-3d-printing-market-they-havent/`.
69 J. R. Windmiller and J. Wang, *Electroanalysis*, 2013, **25**, 29–46.
70 S.-H. Choa, C.-K. Cho, W.-J. Hwang, K. Tae Eun and H.-K. Kim, *Solar Energy Materials and Solar Cells*, 2011, **95**, 3442–3449.
71 S. Bae, H. Kim, Y. Lee, X. Xu, J.-S. Park, Y. Zheng, J. Balakrishnan, T. Lei, H. Ri Kim, Y. I. Song, Y.-J. Kim, K. S. Kim, B. Özyilmaz, J.-H. Ahn, B. H. Hong and S. Iijima, *Nature Nanotechnology*, 2010, **5**, 574–578.
72 J. Noh, D. Yeom, C. Lim, H. Cha, J. Han, J. Kim, Y. Park, V. Subramanian and G. Cho, *IEEE Transactions on Electronics Packaging Manufacturing*, 2010, **33**, 275–283.
73 J. Noh, M. Jung, K. Jung, G. Lee, S. Lim, D. Kim, S. Kim, J. M. Tour and G. Cho, *Organic Electronics*, 2011, **12**, 2185–2191.
74 R. A. Potyrailo, A. Burns, C. Surman, D. J. Lee and E. McGinniss, *The Analyst*, 2012, **137**, 2777.
75 R. Liedert, L. K. Amundsen, A. Hokkanen, M. Mäki, A. Aittakorpi, M. Pakanen, J. R. Scherer, R. A. Mathies, M. Kurkinen, S. Uusitalo, L. Hakalahti, T. K. Nevanen, H. Siitari and H. Söderlund, *Lab on a Chip*, 2012, **12**, 333.
76 J.-M. Verilhac, M. Benwadih, A.-L. Seiler, S. Jacob, C. Bory, J. Bablet, M. Heitzman, J. Tallal, L. Barbut, P. Frère, G. Sicard, R. Gwoziecki, I. Chartier, R. Coppard and C. Serbutoviez, *Organic Electronics*, 2010, **11**, 456–462.
77 M.-W. Wang, W.-C. Lin and M.-H. Lee, *Microsystem Technologies*, 2013, **19**, 1753–1759.
78 M. Hösel, R. R. Søndergaard, D. Angmo and F. C. Krebs, *Advanced Engineering Materials*, 2013, **15**, 995–1001.
79 R. Søndergaard, M. Hösel, D. Angmo, T. T. Larsen-Olsen and F. C. Krebs, *Materials Today*, 2012, **15**, 36–49.
80 S. A. Gevorgyan, M. V. Madsen, H. F. Dam, M. Jørgensen, C. J. Fell, K. F. Anderson, B. C. Duck, A. Mescheloff, E. A. Katz, A. Elschner, R. Roesch, H. Hoppe, M. Hermenau, M. Riede and F. C. Krebs, *Solar Energy Materials and Solar Cells*, 2013, **116**, 187–196.
81 N. Espinosa, R. García-Valverde, A. Urbina, F. Lenzmann, M. Manceau, D. Angmo and F. C. Krebs, *Solar Energy Materials and Solar Cells*, 2012, **97**, 3–13.
82 F. C. Krebs, J. Fyenbo and M. Jørgensen, *Journal of Materials Chemistry*, 2010, **20**, 8994–9001.
83 J. E. Carlé, T. R. Andersen, M. Helgesen, E. Bundgaard, M. Jørgensen and F. C. Krebs, *Solar Energy Materials and Solar Cells*, 2013, **108**, 126–128.
84 L. Wengeler, M. Schmitt, K. Peters, P. Scharfer and W. Schabel, *Chemical Engineering and Processing: Process Intensification*, 2013, **68**, 38–44.
85 Z.-Y. Juang, C.-Y. Wu, A.-Y. Lu, C.-Y. Su, K.-C. Leou, F.-R. Chen and C.-H. Tsai, *Carbon*, 2010, **48**, 3169–3174.
86 H. Tamagaki, Y. Ikari and N. Ohba, *Surface and Coatings Technology*, 2014, **241**, 138–141.
87 P. Maury, D. Turkenburg, N. Stroeks, P. Giesen, I. Barbu, E. Meinders, A. van Bremen, N. Iosad, R. van der Werf and H. Onvlee, *Microelectronic Engineering*, 2011, **88**, 2052–2055.
88 T. Mäkelä, T. Haatainen and J. Ahopelto, *Microelectronic Engineering*, 2011, **88**, 2045–2047.
89 C.-E. Lue, I.-S. Wang, C.-H. Huang, Y.-T. Shiao, H.-C. Wang, C.-M. Yang, S.-H. Hsu, C.-Y. Chang, W. Wang and C.-S. Lai, *Microelectronics Reliability*, 2012, **52**, 1651–1654.
90 J.-T. Wu, S. L.-C. Hsu, M.-H. Tsai, Y.-F. Liu and W.-S. Hwang, *Journal of Materials Chemistry*, 2012, **22**, 15599–15605.
91 J. Perelaer and U. S. Schubert, *Journal of Materials Research*, 2013, **28**, 564–573.
92 J. Perelaer, R. Jani, M. Grouchko, A. Kamyshny, S. Magdassi and U. S. Schubert, *Advanced Materials*, 2012, **24**, 3993–3998.
93 J. Wang, R. C. Y. Auyeung, H. Kim, N. A. Charipar and A. Piqué, *Advanced Materials*, 2010, **22**, 4462–4466.
94 M. Walther, A. Ortner, H. Meier, U. LÃffelmann, P. J. Smith and J. G. Korvink, *Applied Physics Letters*, 2009, **95**, 251107.
95 J. Li, F. Ye, S. Vaziri, M. Muhammed, M. C. Lemme and M. Östling, *Advanced Materials*, 2013, **25**, 3985–3992.
96 R. P. Tortorich and J.-W. Choi, *Nanomaterials*, 2013, **3**, 453–468.
97 S. Park, M. Vosguerichian and Z. Bao, *Nanoscale*, 2013, **5**, 1727–1752.
98 L. Fan, N. Zhang and K. Sun, *Chemical Communications*, 2014, **50**, 6789–6792.
99 M. Layani, P. Darmawan, W. L. Foo, L. Liu, A. Kamyshny, D. Mandler, S. Magdassi and P. S. Lee, *Nanoscale*, 2014, **6**, 4572–4576.
100 T. K. Sau and A. L. Rogach, *Advanced Materials*, 2010, **22**, 1781–1804.
101 S. Iravani, *Green Chemistry*, 2011, **13**, 2638–2650.
102 C. Vollmer and C. Janiak, *Coordination Chemistry Reviews*, 2011, **255**, 2039–2057.
103 A. Guerrero-Martínez, S. Barbosa, I. Pastoriza-Santos and L. M. Liz-Marzán, *Current Opinion in Colloid & Interface Science*, 2011, **16**, 118–127.
104 R. Ghosh Chaudhuri and S. Paria, *Chemical Reviews*, 2012, **112**, 2373–2433.
105 K. N. Thakkar, S. S. Mhatre and R. Y. Parikh, *Nanomedicine: Nanotechnology, Biology and Medicine*, 2010, **6**, 257–262.

106 D. Yang, J. Ma, M. Gao, M. Peng, Y. Luo, W. Hui, C. Chen, Z. Wang and Y. Cui, *RSC Advances*, 2013, **3**, 9681–9686.
107 W. Shen, X. Zhang, Q. Huang, Q. Xu and W. Song, *Nanoscale*, 2014, **6**, 1622–1628.
108 Y. Zhang, P. Zhu, G. Li, T. Zhao, X. Fu, R. Sun, F. Zhou and C.-p. Wong, *ACS Applied Materials & Interfaces*, 2014, **6**, 560–567.
109 A. Feltrin and A. Freundlich, *Renewable Energy*, 2008, **33**, 180–185.
110 D. Cohen, *New Scientist*, 2007, **194**, 34–41.
111 T. Minami, *Thin Solid Films*, 2008, **516**, 5822–5828.
112 *Transparent Electronics*, ed. A. Facchetti and T. Marks, John Wiley & Sons, Ltd, 2010.
113 C.-N. Chen, T.-Y. Dong, T.-C. Chang, M.-C. Chen, H.-L. Tsai and W.-S. Hwang, *Journal of Materials Chemistry C*, 2013, **1**, 5161–5168.
114 Y. Tao, Y. Tao, B. Wang, L. Wang and Y. Tai, *Nanoscale Research Letters*, 2013, **8**, 1–6.
115 F. Molina-Lopez, D. Briand and N. F. de Rooij, *Sensors and Actuators B: Chemical*, 2013, **189**, 89–96.
116 A. Rivadeneyra, J. Fernández-Salmerón, M. Agudo, J. A. López-Villanueva, L. F. Capitan-Vallvey and A. J. Palma, *Sensors and Actuators B: Chemical*, 2014, **195**, 123–131.
117 I. Jung, K. Shin, N. R. Kim and H. M. Lee, *Journal of Materials Chemistry C*, 2013, **1**, 1855–1862.
118 V. Bromberg, S. Ma, F. D. Egitto and T. J. Singler, *Journal of Materials Chemistry C*, 2013, **1**, 6842–6849.
119 M. Abulikemu, E. H. Da'as, H. Haverinen, D. Cha, M. A. Malik and G. E. Jabbour, *Angewandte Chemie*, 2014, **126**, 430–433.
120 E. Butovsky, I. Perelshtein, I. Nissan and A. Gedanken, *Advanced Functional Materials*, 2013, **23**, 5794–5799.
121 P. Buffat and J.-P. Borel, *Physical Review A*, 1976, **13**, 2287–2298.
122 P. R. Couchman and W. A. Jesser, *Nature*, 1977, **269**, 481–483.
123 S. R. Challa, A. T. Delariva, T. W. Hansen, S. Helveg, J. Sehested, P. L. Hansen, F. Garzon and A. K. Datye, *Journal of the American Chemical Society*, 2011, **133**, 20672–20675.
124 R. Ouyang, J.-X. Liu and W.-X. Li, *Journal of the American Chemical Society*, 2013, **135**, 1760–1771.
125 I. Kim, T.-M. Lee and J. Kim, *Journal of Alloys and Compounds*, 2014, **596**, 158–163.
126 D. Tobjörk, H. Aarnio, P. Pulkkinen, R. Bollström, A. Määttänen, P. Ihalainen, T. Mäkelä, J. Peltonen, M. Toivakka, H. Tenhu and R. Österbacka, *Thin Solid Films*, 2012, **520**, 2949–2955.
127 J. West, M. Carter, S. Smith and J. Sears, in *Photonic Sintering of Silver Nanoparticles: Comparison of Experiment and Theory*, ed. V. Shatokha, InTech, 2012.
128 Y. Galagan, E. W. C. Coenen, R. Abbel, T. J. van Lammeren, S. Sabik, M. Barink, E. R. Meinders, R. Andriessen and P. W. M. Blom, *Organic Electronics*, 2013, **14**, 38–46.
129 Z. A. Munir, U. Anselmi-Tamburini and M. Ohyanagi, *Journal of Materials Science*, 2006, **41**, 763–777.
130 M. L. Allen, M. Aronniemi, T. Mattila, A. Alastalo, K. Ojanperä, M. Suhonen and H. Seppä, *Nanotechnology*, 2008, **19**, 175201.
131 J. Perelaer, B.-J. deGans and U. S. Schubert, *Advanced Materials*, 2006, **18**, 2101–2104.
132 R. Roy, D. Agrawal, J. Cheng and S. Gedevanishvili, *Nature*, 1999, **399**, 668–670.
133 J. Niittynen, R. Abbel, M. Mäntysalo, J. Perelaer, U. S. Schubert and D. Lupo, *Thin Solid Films*, 2014, **556**, 452–459.
134 M. Neophytou, E. Georgiou, M. M. Fyrillas and S. A. Choulis, *Solar Energy Materials and Solar Cells*, 2014, **122**, 1–7.
135 S.-H. Park, S. Jang, D.-J. Lee, J. Oh and H.-S. Kim, *Journal of Micromechanics and Microengineering*, 2013, **23**, 015013.
136 Y.-I. Lee, S. Kim, S.-B. Jung, N. V. Myung and Y.-H. Choa, *ACS Applied Materials & Interfaces*, 2013, **5**, 5908–5913.
137 S. Magdassi, M. Grouchko, O. Berezin and A. Kamyshny, *ACS Nano*, 2010, **4**, 1943–1948.
138 M. Layani, M. Gruchko, O. Milo, I. Balberg, D. Azulay and S. Magdassi, *ACS Nano*, 2009, **3**, 3537–3542.
139 J. J. P. Valeton, K. Hermans, C. W. M. Bastiaansen, D. J. Broer, J. Perelaer, U. S. Schubert, G. P. Crawford and P. J. Smith, *Journal of Materials Chemistry*, 2009, **20**, 543–546.
140 K. Kordás, T. Mustonen, G. Tóth, H. Jantunen, M. Lajunen, C. Soldano, S. Talapatra, S. Kar, R. Vajtai and P. Ajayan, *Small*, 2006, **2**, 1021–1025.
141 V. Dua, S. Surwade, S. Ammu, S. Agnihotra, S. Jain, K. Roberts, S. Park, R. Ruoff and S. Manohar, *Angewandte Chemie International Edition*, 2010, **49**, 2154–2157.
142 N. Behabtu, J. R. Lomeda, M. J. Green, A. L. Higginbotham, A. Sinitskii, D. V. Kosynkin, D. Tsentalovich, A. N. G. Parra-Vasquez, J. Schmidt, E. Kesselman, Y. Cohen, Y. Talmon, J. M. Tour and M. Pasquali, *Nature Nanotechnology*, 2010, **5**, 406–411.
143 F. Torrisi, T. Hasan, W. Wu, Z. Sun, A. Lombardo, T. S. Kulmala, G.-W. Hsieh, S. Jung, F. Bonaccorso, P. J. Paul, D. Chu and A. C. Ferrari, *ACS Nano*, 2012, **6**, 2992–3006.
144 D. Parviz, S. Das, H. S. T. Ahmed, F. Irin, S. Bhattacharia and M. J. Green, *ACS Nano*, 2012, **6**, 8857–8867.
145 M. Boccard, C. Battaglia, S. Hänni, K. Söderström, J. Escarré, S. Nicolay, F. Meillaud, M. Despeisse and C. Ballif, *Nano Letters*, 2012, **12**, 1344–1348.
146 R. Baetens, B. P. Jelle and A. Gustavsen, *Solar Energy Materials and Solar Cells*, 2010, **94**, 87–105.
147 K. Ellmer, *Nature Photonics*, 2012, **6**, 809–817.
148 *Transparent conductive zinc oxide: basics and applications in thin film solar cells*, ed. K. Ellmer, A. Klein and B. Rech, Springer, Berlin, 2008.
149 Y. Xu, I. Hennig, D. Freyberg, A. James Strudwick, M. Georg Schwab, T. Weitz and K. Chih-Pei Cha, *Journal of Power Sources*, 2014, **248**, 483–488.
150 X. Chen, B. Jia, Y. Zhang and M. Gu, *Light: Science & Applications*, 2013, **2**, e92.
151 R. Giardi, S. Porro, A. Chiolerio, E. Celasco and M. Sangermano, *Journal of Materials Science*, 2013, **48**, 1249–1255.
152 L. T. Le, M. H. Ervin, H. Qiu, B. E. Fuchs and W. Y. Lee, *Electrochemistry Communications*, 2011, **13**, 355–358.
153 E. B. Secor, P. L. Prabhumirashi, K. Puntambekar, M. L. Geier and M. C. Hersam, *The Journal of Physical Chemistry Letters*, 2013, **4**, 1347–1351.
154 Y. Su, J. Du, D. Sun, C. Liu and H. Cheng, *Nano Research*, 2013, **6**, 842–852.
155 J. Jang, Y. Yoon, H. Jeong, H. Lee, Y. Song, K. Cho, S. Hong, H. Lee and T. Lee, *Thin Solid Films*, 2013, **542**, 327–331.
156 G.-W. Huang, H.-M. Xiao and S.-Y. Fu, *Nanoscale*, 2014.
157 J.-A. Jeong and H.-K. Kim, *Applied Physics Letters*, 2014, **104**, 071906.
158 J.-A. Jeong, H.-K. Kim and J. Kim, *Solar Energy Materials and Solar Cells*, 2014, **125**, 113–119.
159 J.-A. Jeong, Y.-J. Jeon, S.-S. Kim, B. Kyoung Kim, K.-B. Chung and H.-K. Kim, *Solar Energy Materials and Solar Cells*, 2014, **122**, 241–250.
160 P. Chen, H. Chen, J. Qiu and C. Zhou, *Nano Research*, 2010, **3**, 594–603.
161 L. Xie, Y. Feng, M. Mantysalo, Q. Chen and L.-R. Zheng, *IEEE Sensors Journal*, 2013, **13**, 3948–3956.
162 D. Janas and K. K. Koziol, *Nanoscale*, 2014, **6**, 3037–3045.
163 S. Hurch, H. Nolan, T. Hallam, N. C. Berner, N. McEvoy and G. S. Duesberg, *Carbon*, 2014, **71**, 332–337.
164 Y.-F. Liu, M.-H. Tsai, Y.-F. Pai and W.-S. Hwang, *Applied Physics A*, 2013, **111**, 509–516.
165 C. Liu, Y. Xu, Z. Liu, H. N. Tsao, K. MÃŒllen, T. Minari, Y.-Y. Noh and H. Sirringhaus, *Organic Electronics*, 2014.
166 M.-C. Hsieh, C. Kim, M. Nogi and K. Suganuma, *Nanoscale*, 2013, **5**,

9289–9295.

167 A. Määttänen, U. Vanamo, P. Ihalainen, P. Pulkkinen, H. Tenhu, J. Bobacka and J. Peltonen, *Sensors and Actuators B: Chemical*, 2013, **177**, 153–162.

168 A. Maza, B. Cook, G. Jabbour and A. Shamim, *IET Microwaves, Antennas Propagation*, 2012, **6**, 1366–1373.

169 J. J. Adams, E. B. Duoss, T. F. Malkowski, M. J. Motala, B. Y. Ahn, R. G. Nuzzo, J. T. Bernhard and J. A. Lewis, *Advanced Materials*, 2011, **23**, 1335–1340.

170 B. S. Cook, Y. Fang, S. Kim, T. Le, W. B. Goodwin, K. H. Sandhage and M. M. Tentzeris, *Electronic Materials Letters*, 2013, **9**, 669–676.

171 C.-H. Ko, *Automation in Construction*, 2010, **19**, 588–595.

172 J. Virtanen, J. Virkki, L. Sydanheimo, M. Tentzeris and L. Ukkonen, *IEEE Transactions on Automation Science and Engineering*, 2013, **10**, 796–806.

173 B. Cook, T. Le, S. Palacios, A. Traille and M. Tentzeris, *IEEE Microwave Magazine*, 2013, **14**, 103–114.

174 S. Kim, C. Mariotti, F. Alimenti, P. Mezzanotte, A. Georgiadis, A. Collado, L. Roselli and M. Tentzeris, *IEEE Microwave Magazine*, 2013, **14**, 66–77.

175 M. Schneider, A. Türke, W.-J. Fischer and P. A. Kilmartin, *Food Chemistry*, 2014, **159**, 428–432.

176 L. B. Kong and H. Huang, in *Thin Film Gas Sensors Based on Nanocarbon Materials*, ed. S. Li, J. Wu, Z. M. Wang and Y. Jiang, Springer International Publishing, 2013, pp. 189–223.

177 L. Yang, R. Vyas, A. Rida, J. Pan and M. Tentzeris, Electronic Components and Technology Conference, 2008. ECTC 2008. 58th, 2008, pp. 2156–2159.

178 B. Cook, J. Cooper and M. Tentzeris, *IEEE Transactions on Microwave Theory and Techniques*, 2013, **61**, 4714–4723.

179 S. M. Z. Hossain, R. E. Luckham, A. M. Smith, J. M. Lebert, L. M. Davies, R. H. Pelton, C. D. M. Filipe and J. D. Brennan, *Analytical Chemistry*, 2009, **81**, 5474–5483.

180 C. Shemelya, F. Cedillos, E. Aguilera, E. Maestas, J. Ramos, D. Espalin, D. Muse, R. Wicker and E. Macdonald, 2013 IEEE Sensors, 2013, pp. 1–4.

181 S. B. Kesner and R. D. Howe, *IEEE/ASME transactions on mechatronics : a joint publication of the IEEE Industrial Electronics Society and the ASME Dynamic Systems and Control Division*, 2011, **16**, 1–5.

182 B. Y. Ahn, E. B. Duoss, M. J. Motala, X. Guo, S.-I. Park, Y. Xiong, J. Yoon, R. G. Nuzzo, J. A. Rogers and J. A. Lewis, *Science*, 2009, **323**, 1590–1593.

183 M.-G. Kang, H. Joon Park, S. Hyun Ahn and L. Jay Guo, *Solar Energy Materials and Solar Cells*, 2010, **94**, 1179–1184.

184 M.-Y. Lee, M.-W. Lee, J.-E. Park, J.-S. Park and C.-K. Song, *Microelectronic Engineering*, 2010, **87**, 1922–1926.

185 S. Kim, S. H. Im and S.-W. Kim, *Nanoscale*, 2013, **5**, 5205–5214.

186 H. M. Haverinen, R. A. Myllylä and G. E. Jabbour, *Journal of Display Technology*, 2010, **6**, 87–89.

187 N. A. Harun, M. J. Benning, B. R. Horrocks and D. A. Fulton, *Nanoscale*, 2013, **5**, 3817–3827.

188 M. Singh, H. S. Chae, J. D. Froehlich, T. Kondou, S. Li, A. Mochizuki and G. E. Jabbour, *Soft Matter*, 2009, **5**, 3002.

189 M. Singh, H. S. Chae, J. D. Froehlich, T. Kondou, S. Li, A. Mochizuki and G. Jabbour, *MRS Online Proceedings Library*, 2009, **1197**, 1197–D04–23.

190 P. Wang, S. M. Zakeeruddin, P. Comte, I. Exnar and M. Grätzel, *Journal of the American Chemical Society*, 2003, **125**, 1166–1167.

191 S. Ito, P. Chen, P. Comte, M. K. Nazeeruddin, P. Liska, P. Péchy and M. Grätzel, *Progress in Photovoltaics: Research and Applications*, 2007, **15**, 603–612.

192 S. K. Hau, H.-L. Yip, N. S. Baek, J. Zou, K. O'Malley and A. K.-Y. Jen, *Applied Physics Letters*, 2008, **92**, 253301.

193 J. Kukkola, E. Jansson, A. Popov, J. Lappalainen, J. Mäklin, N. Halonen, G. Tóth, A. Shchukarev, J. P. Mikkola, H. Jantunen, K. Kordás, J. Hast, T. Hassinen, A. Sunnari, K. Jokinen, H. Haverinen, R. Sliz, G. Jabbour, T. Fabritius, R. Myllylä, A. Vasiliev and N. Zaretskiy, *Procedia Engineering*, 2011, **25**, 896–899.

194 P. V. Kamat, *The Journal of Physical Chemistry Letters*, 2013, **4**, 908–918.

195 M. Grätzel, AIP Conference Proceedings, 2013, pp. 59–63.

196 F. Sauvage, M. K. Nazeeruddin and M. Grätzel, in *Metal-Oxide Nanoparticles for Dye-Sensitized Solar Cells*, ed. S. B. Ogale, T. V. Venkatesan and r. G. Blamire, Wiley-VCH Verlag GmbH & Co. KGaA, 2013, pp. 339–383.

197 R. Ahmad, M. Vaseem, N. Tripathy and Y.-B. Hahn, *Analytical Chemistry*, 2013, **85**, 10448–10454.

198 H.-Y. Jin, J.-Y. Kim, J. A. Lee, K. Lee, K. Yoo, D.-K. Lee, B. Kim, J. Y. Kim, H. Kim, H. J. Son, J. Kim, J. A. Lim and M. J. Ko, *Applied Physics Letters*, 2014, **104**, 143902.

199 A. Karpinski, S. Berson, H. Terrisse, M. Mancini-Le Granvalet, S. Guillerez, L. Brohan and M. Richard-Plouet, *Solar Energy Materials and Solar Cells*, 2013, **116**, 27–33.

200 C.-L. Chen, T.-W. Chang, S.-C. Su, H. Teng and Y.-L. Lee, *Journal of Power Sources*, 2014, **247**, 406–411.

201 M. Zhu, L. Chen, H. Gong, M. Zi and B. Cao, *Ceramics International*, 2014, **40**, 2337–2342.

202 W.-Q. Wu, Y.-F. Xu, H.-S. Rao, C.-Y. Su and D.-B. Kuang, *Nanoscale*, 2013, **5**, 4362–4369.

203 M. Černá, M. Veselý, P. Dzik, C. Guillard, E. Puzenat and M. Lepičová, *Applied Catalysis B: Environmental*, 2013, **138–139**, 84–94.

204 C. Dong, W. Xiang, F. Huang, D. Fu, W. Huang, U. Bach, Y.-B. Cheng, X. Li and L. Spiccia, *Nanoscale*, 2014, **6**, 3704–3711.

205 D. Zhang, T. Yoshida, T. Oekermann, K. Furuta and H. Minoura, *Advanced Functional Materials*, 2006, **16**, 1228–1234.

206 M. I. Dar, A. K. Chandiran, M. Grätzel, M. K. Nazeeruddin and S. A. Shivashankar, *Journal of Materials Chemistry A*, 2014, **2**, 1662–1667.

207 D. H. Kim, W. M. Seong, I. J. Park, E.-S. Yoo, S. S. Shin, J. S. Kim, H. S. Jung, S. Lee and K. S. Hong, *Nanoscale*, 2013, **5**, 11725–11732.

208 J. Chang, Y. Ning, S. Wu, W. Niu and S. Zhang, *Advanced Functional Materials*, 2013, **23**, 5910–5915.

209 A. M. Cant, F. Huang, X. L. Zhang, Y. Chen, Y.-B. Cheng and R. Amal, *Nanoscale*, 2014, **6**, 3875–3880.

210 R. Sliz, Y. Suzuki, A. Nathan, R. Myllyla and G. Jabbour, author, 2012, pp. 84771G–84771G–6.

211 C. Jiang, R. Wang and B. A. Parkinson, *ACS Combinatorial Science*, 2013, **15**, 639–645.

212 J. Kwon, S. Hong, H. Lee, J. Yeo, S. S. Lee and S. H. Ko, *Nanoscale Research Letters*, 2013, **8**, 1–6.

213 G. Yang, Q. Wang, C. Miao, Z. Bu and W. Guo, *Journal of Materials Chemistry A*, 2013, **1**, 3112–3117.

214 M. Fang, W. Voit, Y. Wu, L. Belova and K. Rao, *MRS Online Proceedings Library*, 2013, **1547**, 13–20.

215 Y.-H. Choi, D.-H. Kim, H. S. Han, S. Shin, S.-H. Hong and K. S. Hong, *Langmuir*, 2014, **30**, 700–709.

216 C. Y. Neo and J. Ouyang, *Journal of Power Sources*, 2013, **222**, 161–168.

217 S. Gullapalli, J. M. Grider, H. G. Bagaria, K.-S. Lee, M. Cho, V. L. Colvin, G. E. Jabbour and M. S. Wong, *Nanotechnology*, 2012, **23**, 495605.

218 B. El Zein, M. Abulikemu, S. Boulfrad, R. Sougrat, E. Dogheche and G. Jabbour, European Materials Research Society Spring Meeting, E-MRS Spring 2013, Symposium D - Advanced inorganic materials and structures for photovoltaics, 2013.

219 N. D. Bronstein, L. Li, L. Xu, Y. Yao, V. E. Ferry, A. P. Alivisatos and R. G. Nuzzo, *ACS Nano*, 2014, **8**, 44–53.

220 D.-C. Nguyen, K. Fukatsu, K. Tanimoto, S. Ikeda, M. Matsumura and S. Ito, *International Journal of Photoenergy*, 2013, **2013**, e416245.

221 I. Klugius, R. Miller, A. Quintilla, T. M. Friedlmeier, D. Blázquez-Sánchez, E. Ahlswede and M. Powalla, *Thin Solid Films*, 2013, **535**, 107–111.

222 S. Boulfrad, M. Cassidy, E. Djurado, J. T. S. Irvine and G. Jabbour, *International Journal of Hydrogen Energy*, 2013, **38**, 9519–9524.

223 S. M. Olhero, L. Garcia-Gancedo, T. W. Button, F. J. Alves and J. M. F. Ferreira, *Journal of the European Ceramic Society*, 2012, **32**, 1067–1075.

224 O. Noshchenko, D. Kuscer, O. C. Mocioiu, M. Zaharescu, M. Bele and B. Malič, *Journal of the European Ceramic Society*, 2014, **34**, 297–305.

225 M. Lejeune, T. Chartier, C. Dossou-Yovo and R. Noguera, *Journal of the European Ceramic Society*, 2009, **29**, 905–911.

226 Y. Wei, R. Torah, K. Yang, S. Beeby and J. Tudor, *Smart Materials and Structures*, 2014, **23**, 025034.

227 M. Segal, M. Singh, K. Rivoire, S. Difley, T. Van Voorhis and M. A. Baldo, *Nature Materials*, 2007, **6**, 374–378.

228 M. Segal, C. Mulder, K. Celebi, M. Singh, K. Rivoire, S. Difley, T. Van Voorhis and M. A. Baldo, *Proc. SPIE*, 2008, **6999**, 699912–699912–17.

229 H. Gorter, M. J. J. Coenen, M. W. L. Slaats, M. Ren, W. Lu, C. J. Kuijpers and W. A. Groen, *Thin Solid Films*, 2013, **532**, 11–15.

230 Y. Yoshioka and G. E. Jabbour, *Advanced Materials*, 2006, **18**, 1307–1312.

231 O. Pabst, J. Perelaer, E. Beckert, U. S. Schubert, R. Eberhardt and A. Tünnermann, *Organic Electronics*, 2013, **14**, 3423–3429.

232 D. Mao, I. Mejia, A. Salas-Villasenor, M. Singh, H. Stiegler, B. Gnade and M. Quevedo-Lopez, *Organic Electronics*, 2013, **14**, 505–510.

233 Y. Zhang, J. Stringer, R. Grainger, P. J. Smith and A. Hodzic, *physica status solidi (RRL) – Rapid Research Letters*, 2014, **8**, 56–60.

234 Y. Zhang, J. Stringer, R. Grainger, P. J. Smith and A. Hodzic, *Journal of Composite Materials*, 2014, 0021998314533715.

235 J. K. Mapel, M. Singh, M. A. Baldo and K. Celebi, *Applied Physics Letters*, 2007, **90**, 121102.

236 T. D. Heidel, J. K. Mapel, M. Singh, K. Celebi and M. A. Baldo, *Applied Physics Letters*, 2007, **91**, 093506.

237 T. D. Heidel, J. K. Mapel, K. Celebi, M. Singh and M. A. Baldo, *Proc. SPIE*, 2007, **6656**, 66560I–66560I–9.

238 C. N. Hoth, P. Schilinsky, S. A. Choulis, S. Balasubramanian and C. J. Brabec, in *Solution-Processed Organic Photovoltaics*, ed. E. Cantatore, Springer US, 2013, pp. 27–56.

239 A. Garcia, N. Hanifi, B. Jousselme, P. Jégou, S. Palacin, P. Viel and T. Berthelot, *Advanced Functional Materials*, 2013, **23**, 3668–3674.

240 S. Fathi, P. Dickens, K. Khodabakhshi and M. Gilbert, *Journal of Manufacturing Science and Engineering*, 2013, **135**, 011009–011009.

241 H. Kobayashi, S. Hirata and M. Vacha, *The Journal of Physical Chemistry Letters*, 2013, **4**, 2591–2596.

242 B. Weng, A. Morrin, R. Shepherd, K. Crowley, A. J. Killard, P. C. Innis and G. G. Wallace, *Journal of Materials Chemistry B*, 2014, **2**, 793–799.

243 T. Hibbard, K. Crowley and A. J. Killard, *Analytica Chimica Acta*, 2013, **779**, 56–63.

244 K. Crowley, M. R. Smyth, A. J. Killard and A. Morrin, *Chemical Papers*, 2013, **67**, 771–780.

245 M. M. Eissa, M. Mahbubor Rahman, N. Zine, N. Jaffrezic, A. Errachid, H. Fessi and A. Elaissari, *Acta Biomaterialia*, 2013, **9**, 5573–5582.

246 T. Akagi, T. Fujiwara and M. Akashi, *Langmuir*, 2014, **30**, 1669–1676.

247 T. Soga, Y. Jimbo, K. Suzuki and D. Citterio, *Analytical Chemistry*, 2013, **85**, 8973–8978.

248 R. Tang and X. Feng, *Canadian Chemical Transactions*, 2013, **1**, 78–84.

249 N. Tran and T. J. Webster, *Wiley Interdisciplinary Reviews: Nanomedicine and Nanobiotechnology*, 2009, **1**, 336–351.

250 U. Gbureck, T. Hölzel, U. Klammert, K. Würzler, F. A. Müller and J. E. Barralet, *Advanced Functional Materials*, 2007, **17**, 3940–3945.

251 D. Tadic and M. Epple, *Biomaterials*, 2004, **25**, 987–994.

252 L. Moroni, R. Schotel, J. Sohier, J. R. de Wijn and C. A. van Blitterswijk, *Biomaterials*, 2006, **27**, 5918–5926.

253 B. Leukers, H. Gülkan, S. H. Irsen, S. Milz, C. Tille, M. Schieker and H. Seitz, *Journal of Materials Science: Materials in Medicine*, 2005, **16**, 1121–1124.

254 A. Butscher, M. Bohner, N. Doebelin, S. Hofmann and R. Müller, *Acta Biomaterialia*, 2013, **9**, 9149–9158.

255 B. Derby, *Science*, 2012, **338**, 921–926.

256 M. N. Cooke, J. P. Fisher, D. Dean, C. Rimnac and A. G. Mikos, *Journal of Biomedical Materials Research Part B: Applied Biomaterials*, 2003, **64B**, 65–69.

257 H. Seitz, W. Rieder, S. Irsen, B. Leukers and C. Tille, *Journal of Biomedical Materials Research Part B: Applied Biomaterials*, 2005, **74B**, 782–788.

258 S. J. Hollister, *Nature Materials*, 2005, **4**, 518–524.

259 J. A. Inzana, D. Olvera, S. M. Fuller, J. P. Kelly, O. A. Graeve, E. M. Schwarz, S. L. Kates and H. A. Awad, *Biomaterials*, 2014, **35**, 4026–4034.

260 N. Annabi, A. Tamayol, J. A. Uquillas, M. Akbari, L. E. Bertassoni, C. Cha, G. Camci-Unal, M. R. Dokmeci, N. A. Peppas and A. Khademhosseini, *Advanced Materials*, 2014, **26**, 85–124.

261 D. F. Duarte Campos, A. Blaeser, M. Weber, J. Jäkel, S. Neuss, W. Jahnen-Dechent and H. Fischer, *Biofabrication*, 2013, **5**, 015003.

262 V. Mironov, T. Boland, T. Trusk, G. Forgacs and R. R. Markwald, *Trends in Biotechnology*, 2003, **21**, 157–161.

263 E. Sachlos, D. Gotora and J. T. Czernuszka, *Tissue Engineering*, 2006, **12**, 2479–2487.

264 W.-Y. Yeong, C.-K. Chua, K.-F. Leong, M. Chandrasekaran and M.-W. Lee, *Rapid Prototyping Journal*, 2006, **12**, 229–237.

265 C. Z. Liu, Z. D. Xia, Z. W. Han, P. A. Hulley, J. T. Triffitt and J. T. Czernuszka, *Journal of Biomedical Materials Research Part B: Applied Biomaterials*, 2008, **85B**, 519–528.

266 D. N. Silva, M. Gerhardt de Oliveira, E. Meurer, M. I. Meurer, J. V. Lopes da Silva and A. Santa-Bárbara, *Journal of Cranio-Maxillofacial Surgery*, 2008, **36**, 443–449.

267 M. S. Mannoor, Z. Jiang, T. James, Y. L. Kong, K. A. Malatesta, W. O. Soboyejo, N. Verma, D. H. Gracias and M. C. McAlpine, *Nano Letters*, 2013, **13**, 2634–2639.

268 R. Critchley, I. Corni, J. A. Wharton, F. C. Walsh, R. J. K. Wood and K. R. Stokes, *Advanced Engineering Materials*, 2013, **15**, 980–985.

269 L. Ionov, *Advanced Functional Materials*, 2013, **23**, 4555–4570.

270 S. V. Murphy, A. Skardal and A. Atala, *Journal of Biomedical Materials Research Part A*, 2013, **101A**, 272–284.

271 Y. Tan, D. J. Richards, T. C. Trusk, R. P. Visconti, M. J. Yost, M. S. Kindy, C. J. Drake, W. S. Argraves, R. R. Markwald and Y. Mei, *Biofabrication*, 2014, **6**, 024111.

272 T. Boland, T. Xu, B. Damon and X. Cui, *Biotechnology Journal*, 2006, **1**, 910–917.

273 A. Pfister, R. Landers, A. Laib, U. Hübner, R. Schmelzeisen and R. Mülhaupt, *Journal of Polymer Science Part A: Polymer Chemistry*, 2004, **42**, 624–638.

274 T. Xu, C. A. Gregory, P. Molnar, X. Cui, S. Jalota, S. B. Bhaduri and T. Boland, *Biomaterials*, 2006, **27**, 3580–3588.

275 T. Xu, J. Jin, C. Gregory, J. J. Hickman and T. Boland, *Biomaterials*, 2005, **26**, 93–99.

276 J. L. Connell, E. T. Ritschdorff, M. Whiteley and J. B. Shear, *Proceedings of the National Academy of Sciences*, 2013, 201309729.

277 J.-U. Park, J. H. Lee, U. Paik, Y. Lu and J. A. Rogers, *Nano Letters*, 2008, **8**, 4210–4216.

278 O. Paris, G. Fritz-Popovski, D. Van Opdenbosch and C. Zollfrank, *Advanced Functional Materials*, 2013, **23**, 4408–4422.
279 P. K. Vemula, N. Wiradharma, J. A. Ankrum, O. R. Miranda, G. John and J. M. Karp, *Current Opinion in Biotechnology*, 2013, **24**, 1174–1182.
280 J. Aizenberg and P. Fratzl, *Advanced Functional Materials*, 2013, **23**, 4398–4399.
281 M. J. N. Pereira, I. F. Carvalho, J. M. Karp and L. S. Ferreira, *Journal of Cardiovascular Translational Research*, 2011, **4**, 616–630.
282 M. Castilho, C. Moseke, A. Ewald, U. Gbureck, J. Groll, I. Pires, J. Teßmar and E. Vorndran, *Biofabrication*, 2014, **6**, 015006.

